Climate shapes the geographic distribution and introgressive spread of color ornamentation in common wall lizards

Maravillas Ruiz Miñano[1,2], Geoffrey M. While[2], Weizhao Yang[1], Christopher P. Burridge[2], Roberto Sacchi[3], Marco Zuffi[4], Stefano Scali[5], Daniele Salvi,[6] & Tobias Uller[1]

1. Department of Biology, Lund University, Sölvegatan 37, 223 62 Lund, Sweden

2. School of Biological Sciences, University of Tasmania, Hobart, Tasmania 7005, Australia

3. Department of Earth and Environmental Sciences, University of Pavia, Viale Taramelli 24, 27100 Pavia, Italy

4. Museum of Natural History, University of Pisa, via Roma 79, 56011 Calci (Pisa), Italy

5. Museum of Natural History, corso Venezia 55, 20121 Milano, Italy

6. Department of Health, Life and Environmental Sciences, University of L'Aquila, Via Vetoio, 67100 Coppito, L'Aquila, Italy

Article for the *American Naturalist*

Short title: Climate and color ornamentation in lizards

Key words: sexual selection, geographic variation, lizard, introgression, coloration

Word count: approx. 5900 words excluding references, 4 Tables, 3 Figures,

Supplementary Material includes Supplementary Results; Supplementary Tables S1-S7; Supplementary Figures S1-S14

Abstract

Climate can exert an effect on the strength of sexual selection, but empirical evidence is limited. Here, we tested if climate predicts the geographic distribution and introgressive spread of sexually selected male color ornamentation across 114 populations of the common wall lizard, *Podarcis muralis*. Coloration was highly structured across the landscape, and did not reflect genetic differentiation. Instead, color ornamentation was consistently exaggerated in hot and dry environments, suggesting that climate-driven selection maintains geographic variation in spite of gene flow. Introgression of color ornamentation into a distantly related lineage appears to be ongoing and was particularly pronounced in warm climates with wet winters and dry summers. Combined, these results suggest that sexual ornamentation is consistently favored in climates that allow a prolonged reproductive season and high and reliable opportunities for lizard activity. This pattern corroborates theoretical predictions that such climatic conditions reduce the temporal clustering of receptive females and increase male-male competition, resulting in strong sexual selection. In summary, we provide compelling evidence for the importance of climate for the evolution of color ornamentation, and demonstrate that geographic variation in the strength of sexual selection influences introgression of this phenotype.

Introduction

Biologists have known for centuries that species vary across their range, but unravelling the causes of this variation remains a major challenge. Geographic mosaics of phenotypic variation are the result of both historical processes as well as ongoing selection and migration. To identify the putative causes of selection, it is therefore necessary to have detailed knowledge about history, such as population divergence, range expansion and secondary contact. Secondary contact zones in particular provide powerful frameworks to establish if selection contributes to phenotypic variation across the landscape (Barton and Hewitt 1989; Orteu and Jiggins 2020). Occasionally, particular phenotypes and genes introgress from one lineage into another, a phenomenon that can occur when the trait confers an adaptive advantage in the recipient lineage ("adaptive introgression"; Hedrick 2013; Arnold 2016). Thus, concordance between environmental predictors of phenotypic variation within a lineage and environmental predictors of phenotypic introgression between lineages would provide particularly strong evidence that selection is operating, and may help to identify its underlying causes (Uy and Stein 2007).

Climate is a strong candidate for geographic mosaics in selection, including selection on traits involved in competition for sexual partners. Climate commonly influences resource distribution, activity patterns and reproductive cycles, all of which can modulate the strength of sexual selection (Emlen and Oring 1977; Shuster and Wade 2003; Cornwallis and Uller 2010; Macías-Ordóñez et al. 2013; Garcia-Roa et al. 2020). For example, a short activity season with synchronized breeding of females will tend to reduce the opportunity for males to mate multiply, resulting in weak sexual selection (Shuster and Wade 2003). As a result, sexual ornaments, such as the size or intensity of color patches, should be exaggerated in climates that allow intense competition for mates. Climate can also impose demands on the physiological and behavioral traits

that sexual ornaments are supposed to signal (Evans and Gustafsson 2017; Garcia-Roa et al. 2019; Moore et al. 2019). Local adaptation to climate can therefore make coloration uninformative or prohibitively expensive.

Climatic effects on sexual selection are likely to be particularly important for ectotherms, as their physiological functions and reproduction are inherently temperature-dependent (Angilletta 2009; Sinervo et al. 2010). Indeed, temperature has been suggested to be a major driver of spatial and temporal variation in the intensity and form of sexual selection in ectotherms (Garcia-Roa et al. 2020). However, there is a conspicuous lack of empirical evidence that climate maintains variation in sexually selected characters (e.g., McLean et al. 2015; Moore et al. 2019; Rosenthal and Elias 2019; for discussion, see Cornwallis and Uller 2010; Macías-Ordóñez et al. 2013; McLean and Stuart-Fox 2014; Svensson 2019; Garcia-Roa et al. 2020).

Wall lizards (genus *Podarcis*) exhibit striking geographic variation in coloration, which has puzzled naturalists for well over a century (e.g., Eimer 1881; Cyrén 1924). Colors are typically expressed more in males than in females and are known to function as sexual displays in male-male contests (Pérez i de Lanuza et al. 2013). One of the most extreme cases of within-species variation occurs in common wall lizards (*Podarcis muralis*) on the Italian peninsula (Fig. 1). Here, the species varies from the ancestral brown color to an intense green and shows a pronounced variation in black coloration on the throat, chest and belly (see Fig. 1 and Results). Within a population, green and black coloration are more highly expressed in males and positively correlated with each other and with other male traits under intra-sexual selection (e.g., body size and head size; While et al. 2015; Heathcote et al. 2016; MacGregor et al. 2017a). The expression of coloration itself does not appear strongly affected by the environment: phenotypic differences between individuals and populations remain consistent across seasons, in captivity, and in non-

native populations introduced to much cooler climates (e.g., Schulte et al. 2012; While et al. 2015; MacGregor et al. 2017b).

The green-and-black common wall lizard phenotype has been referred to as a distinct subspecies (*P. muralis nigriventris* Bonaparte, 1838), and evolved within what we here refer to as the 'Italian' (IT) lineage of the species (distributed throughout central Italy, Fig. 1; Yang et al. 2018). However, the species' extremes of the phenotype can be found even within this lineage (Yang et al. 2018; see Results). Furthermore, analyses of phenotypic and genomic data have shown that the green-and-black phenotype has introgressed into the distantly related 'Southern Alps' (SA) lineage, despite limited overall gene flow (While et al. 2015; Yang et al. 2018; Yang et al. 2020). Introgression is supported by the close association between phenotypic and genome-wide clines (Yang et al. 2018). Phylogenetic reconstruction of introgressed sequences suggests that the green-and-black phenotype originated in the south of the IT lineage, and subsequently spread northwards to the contact zone between IT and SA lineages, and further into the SA lineage (Yang et al. 2018,2020). Studies of experimental populations demonstrate that the highly asymmetric genetic and phenotypic introgression is a result of green-and-black IT males being behaviorally dominant over the ancestral phenotype, making IT males more likely to hybridize with females of other lineages than *vice versa* (While et al. 2015; Heathcote et al. 2016; MacGregor et al. 2017a).

The geographic variation in common wall lizard coloration, combined with secondary contact and introgression, provide an outstanding opportunity to test for climate-mediated selection. To this end, we first quantify variation in male color ornamentation across the landscape. Second, we determine to what extent phenotypic variation within the Italian lineage can be explained by genetic differentiation or climate. Third, to confirm a role of climate-mediated

selection, we test if the same climatic factors that explain variation within the Italian lineage also can explain the introgressive spread of male color ornamentation into the Southern Alps lineage.

Methods

Study area

Between 2012 and 2018, we collected morphological and coloration data on common wall lizards from 114 locations across central and northern Italy (Table S1; Fig. S1). The sampling covered a broad range of climates, represented by locations from the coast to about 1500 meters above sea level. All populations were visited during the breeding season (from late March until early May) and individuals were captured opportunistically (using noosing) from suitable habitat. Typical habitats of wall lizards include stone walls or concrete structures delimiting gardens, roadsides and agricultural landscapes with walls, fences or other structures, fields with bushes or other features that provide structural complexity, or open forest. Each location includes a variety of habitats, but most commonly centered on a village or human-made structures (e.g., abandoned buildings, rural roads) and the areas surrounding these (e.g., olive plantations, forest). We refer to each of the sampling locations as a 'population'.

Phenotypic data

Upon capture, lizards were measured, and traits were recorded, including snout to vent length (SVL) and total length (both ± 1 mm) with a ruler, and head width and head length (both ±0.01 mm) with a calliper. Body mass (±0.01 g) was recorded using a digital scale. All individuals were then photographed dorsally and ventrally with a Canon EOS 350D digital camera (Canon U.S.A., Inc., Lake Success, NY) using an X-rite Colour-Checker chart as background. Intensity of the

dorsal coloration ("greenness") of each individual was scored in the field by two of the authors (GMW and either TU or MRM) using a scale from 1-10 ('1' being completely brown individuals and '10' representing the most intense green color; While et al. 2015). This scoring is highly repeatable within and across observers and correlates well with spectrophotometry and with scoring from digital photographs (for data and details, see While et al. 2015; MacGregor et al. 2017a). The extent of black ventral coloration ("blackness") was scored from digital photographs by quantifying the proportion of black to non-black pixels on each lizard's chest (While et al. 2015), a variable that ranges from zero to one. We also collected tissue samples from the tail, or toes when the tail was lost, for later DNA extraction. Lizards were released back at their point of capture.

Common wall lizards only develop their green-and-black coloration once they reach maturity and therefore only adult males with an SVL above 50 mm were included in the phenotypic analyses. We calculated the average blackness and greenness for each population, retaining only populations with data on at least five males (see Table S1 for sample sizes for each population). The final phenotype data set consists of 1801 male individuals from 114 populations (Supplementary File 1 and 2).

DNA sequence data

The data set for the phenotypic analyses contains a subset of 71 populations for which we also generated genetic data (for up to seven females and seven males per population) using double-digest RAD-sequencing (ddRAD) on an Illumina HiSeq 2500 platform (Novogene; Hong Kong). The protocol and downstream analyses are explained in detail elsewhere (Yang et al. 2018,2020). In brief, we used STACKS v2.2 to obtain single nucleotide polymorphisms (SNPs) (Catchen et

al. 2013) and mapped clean reads to the reference genome of *P. muralis* (PodMur_1.0; Andrade et al. 2019). One SNP was retained per RAD tag to exclude strongly linked loci in the dataset, SNPs with depth <10 were removed as low- depth loci, and SNPs with depth >95th percentile were removed to avoid PCR duplicates or SNPs from high complexity regions (Fan et al. 2016). The individuals with average depth of coverage for all SNPs <8 were also removed from the whole data set. PLINK (Chang et al. 2015) was used to filter the SNPs with minimum minor allele frequency (MAF) <0.05, deviation from Hardy–Weinberg equilibrium ($p < 0.05$), or with missing rate >0.1 in each population. Finally, we excluded individuals with genotyping rate <90%. After quality filtering, this data set consisted 35,227 SNPs for 896 individuals from 71 populations (Supplementary File 3).

Population genetic analyses

SNPs were used for two purposes. First, we revisited the population genetic structure across the study region (see Yang et al. 2018,2020). We conducted a principal component analysis (PCA) based on genetic distance in Plink v1.9 (Chang et al. 2015). We then used ADMIXTURE v1.3.0 (Alexander et al. 2009) to estimate individual admixture by varying the co-ancestry clusters (K) from 2 to 10. Ten-fold cross-validation was applied to evaluate the fit of the data to different number of clusters. Second, we tested if, within the Italian lineage, differences in male coloration between populations were associated with genetic differentiation. We used multiple matrix regression with randomization (MMRR; Wang 2013) with the Euclidian phenotypic distance for (standardized) greenness and blackness as the dependent matrix. The independent predictors were the genetic (pairwise population F_{ST}) and climatic (Euclidian distances between the two climatic principal components; see below) distances. All distance matrices were standardized (Wang 2013).

These analyses were performed only within the IT lineage, representing individuals with the probability of being assigned to the IT lineage (Q-score) >0.9, as estimated by ADMIXTURE for K=2, and only populations with at least five genotypes.

Climatic variables

We extracted 19 bioclimatic variables from Worldclim 2.0 (Fick 2017) at a 30 arc-sec spatial (1 km^2) resolution for all the sampling locations used in the phenotypic analyses. These bioclimatic variables contain mean, maximum, minimum and seasonality data for both temperature and precipitation (see Table S2), and thus captures information about climatic regimes that influence lizard activity, including its seasonality (e.g., Adolph and Porter 1993; Olsson et al. 2011a). We identified the major climatic axes of variation across these locations using principal component analysis (*ade4* package; Dray and Dufour 2007). The number of retained principal components (PCs) for downstream analyses was calculated using the broken stick method (Legendre and Legendre 2012).

The principal component analysis supported the retention of PC1 and PC2, which explained 79.5 % (55.5% and 24% respectively) of the variation in the 19 climatic variables. The loadings are reported in Table S2. Overall, PC1 represents a gradient from hot and dry (negative values) to cool and wet (positive values) climate, and the geographic distribution of the scores clearly separate out lowland regions from mountains (see Fig. 2a below). PC2 captures seasonal variation in temperature and precipitation. Negative values of PC2 represent locations with mild, relatively wet winters and hot and dry summers. Positive values of PC2 represent locations with higher annual variation in temperature and where both winter and summer seasons experience substantial rainfall (Table S2). This results in a pronounced shift in PC2 from the coast and further

inland (see Fig. 2b below). These PCs reflect well the Köpper-Geigen climate classification map of Italy (Beck et al. 2018; compare Fig. 2a,b with Fig. S2).

Spatial analyses

Phenotypic introgression of greenness and blackness is accompanied by genetic exchange of a very limited part of the genome (Yang et al. 2018). As a result, even individuals and populations that are overwhelmingly (>99.999%) assigned to the Southern Alps lineage on the basis of the >35,000 unlinked SNPs we employ in this study can exhibit highly exaggerated green-and-black coloration (While et al. 2015; Yang et al. 2018, 2020). To test (i) if climate explains the geographic variation in male coloration within the IT lineage, and (ii) if the same climatic conditions explain geographic variation in the introgression of the color phenotypes into the Southern Alps lineage, we therefore classified populations into three categories: Italian (IT; if $Q_{IT} > 0.90$), Southern Alps (SA; if $Q_{IT} < 0.10$), and hybrids ($0.10 \leq Q_{IT} \leq 0.90$). Populations without genetic data were assigned to these categories on the basis of the inferred location of the hybrid zone (see Results and Yang et al. 2020). This resulted in a total of 58 populations assigned to the IT lineage, 37 populations assigned to the SA lineage, and 19 populations assigned to the hybrid zone.

For each of the three categories of populations, our aim was to establish the unique and shared contributions of climate (the focal predictor of selection on color ornamentation), a linear latitudinal and longitudinal trend (expected if the color ornaments originated and spread from the south; Yang et al. 2018), and more complex spatial structure across the landscape (arising from historical and contemporary limits to gene flow and selection).

To this end, we analyzed the spatial phenotypic structure using distance-based Moran eigenvectors maps (dbMEMs). This method is explained by Legendre and Legendre (2012), and

the information required to carry out the analyses in R (using the package *adespatial*; Dray et al. 2012) can be found in Borcard et al. (2018). Briefly, dbMEM variables are the eigenvectors of a spatial matrix calculated from the geographical coordinates of the sampling locations (Dray et al. 2006; Legendre and Legendre 2012). These eigenvectors represent orthogonal spatial descriptors of the variation in the focal traits (e.g., greenness and blackness) across sampling locations at different scales, from broad to fine scale (defined by Moran's I). The eigenvectors can therefore be used as spatial explanatory variables in multiple regression or redundancy analysis (RDA; which is an extension of regression models for multivariate dependent variables). The resulting canonical axes from the RDA represent the spatially structured variation in the focal traits and these can be subject to further analyses, for example, to test if the spatially structured variation can be explained by environmental factors (in this case, climate). Furthermore, it is possible to perform a variation partitioning analyses to quantify both unique and shared fractions of phenotypic variation explained by spatial and environmental (here climatic) predictors. Thus, this provides a comprehensive assessment of the geographic variation in phenotype and the association between phenotype and climate from fine to broad spatial scales.

Following Legendre and Legendre (2012), we first tested for and, if significant, removed any overall linear relationship between phenotype and latitude/longitude by regressing the phenotypic data against population x-y coordinates and retaining the residuals. This ensures that the dbMEMs model spatial structure that cannot simply be captured by a linear association between phenotype and spatial coordinates. A linear trend can arise for several reasons, including spatially restricted gene flow, a cline in environmental conditions, or that the characters originated only recently and spread under (possibly environment-dependent) selection. We subsequently created a geographic distance matrix for all the locations where each location was linked within a

minimum distance using the longest edge in a minimum spanning tree (Fortin and Dale 2005). We first ran a global RDA on the population phenotypic data (average greenness and blackness) and used forward selection to identify significant dbMEMs (Blanchet et al. 2008). These significant dbMEM variables were then used as variables in the final RDA, resulting in one or more canonical axes that represent the spatially structured variation in greenness and blackness. To test if any of this spatial variation in phenotype is explained by climate, the fitted population scores from the significant canonical axes were regressed on the two climatic PCs using a linear model. Statistical significance was assessed using ANOVA. Finally, we performed a variance partitioning analysis (Peres-neto et al. 2006; Legendre and Legendre 2012). This method (implemented in the *vegan* package: Borcard et al. 2018; Oksanen et al. 2019) uses partial redundancy analyses to quantify the unique and shared fractions of the phenotypic variation explained by the linear trend (x,y coordinates), the spatial structure (dbMEMs), and the two climatic PCs. Statistical significance and unique and shared contributions of climate, linear trend, and spatial structure (dbMEM) were determined by ANOVA using 1000 permutations. These spatial analyses and variance partitioning analyses were subsequently repeated for the 43 IT populations for which we had genetic data, which allowed us to add genetic distance as an additional source of the observed phenotypic variation across the landscape. To this end, we calculated pairwise F_{ST} between populations and used a principal coordinate analyses (PCoA) on the dissimilarity matrix (Legendre and Andersson 1999) to obtain ordination axes. The first three axes (retained using the broken stick method) were subsequently used as explanatory variables in partial RDAs and variance partitioning analyses as described above.

Complementary univariate analyses

To complement the multivariate analyses, we ran univariate spatial analyses using Moran eigenvector-based spatial models. This is particularly useful to assess the patterns of introgression, as our measure of green dorsal color is effectively fixed for 'pure' individuals from the Southern Alps lineage (i.e., they all exhibit the brown ancestral state), while the extent of black ventral spotting is variable. Thus, analyzing greenness and blackness separately may reveal patterns that are difficult to discern in a multivariate analysis. As for the multivariate analyses, we ran analyses separately for Italian (IT) lineage, Southern Alps (SA) lineage, and the hybrid zone, using linear random effect regression models that eliminates residual spatial dependence using Moran eigenvectors (Murakami et al. 2017; Murakami and Griffith 2019; implemented using the spmoran package v.0.2.0; Murakami 2020).

Briefly, for each trait (standardized mean greenness or blackness) and data set (IT, SA or hybrids), we use the following steps: (1) test for a linear relationship between the focal trait and latitude/longitude and, when the model was significant, detrend the data; (2) define neighboring populations using the minimum spanning tree and select positive eigenvectors; (3) run a random effects model with the focal trait as dependent variable and climatic PC1 and PC2 as explanatory variables, while controlling for the spatial connectivity with the forward-selected Moran eigenvectors. In addition, this model provides information of the spatial scale of the observed pattern; a scaled Moran's I (i.e., the Moran.I/max(Moran.I) ratio) value close to 1 indicates large-scale spatial structure, while a value close to 0 indicates a local scale spatial structure. Finally, we (4) ran an alternative model that allows the spatial scales of individual covariates of the model (i.e., climatic PC1 and PC2) to vary (Murakami et al. 2017). Spatially varying coefficients were included only if these improved the model fit (i.e., setting x_sel = TRUE), which was assessed

using Aikaike Information Criterion. This approach makes it possible to assess if the climatic dependence varies across the landscape. Such variation would arise, for example, if introgression of green and black coloration is ongoing since it would imply that climate fails to predict the color far away from the secondary contact zone. All the statistical analyses were performed in R v. 3.6.2. Data are deposited in the Dryad Digital Repository, https://doi.org/10.5061/dryad.s1rn8pk7c (Ruiz Miñano et al. 2021).

Results

Population genetic structure

A PCA on the SNP data revealed that the first principal component (variance explained = 73.5%) separated all individuals into two clusters that correspond to the SA and IT lineages, with several intermediate clusters of individuals in between (Fig. 1c). The second principal component (variance explained = 8.1%) reflected the divergence within the IT lineage from north to south. The ADMIXTURE analysis was consistent with PCA when the number of presumed ancestral clusters (K) was set to two (Fig. 1d). Increased K supported the divergence between SA and IT, the hybrid zone, and the within-lineage differentiation (Fig. 1d; Fig. S3). Out of the 71 populations with genetic data, 43 populations were assigned to the Italian lineage ($Q_{IT} > 0.90$), 18 populations were assigned to the Southern Alps lineage ($Q_{IT} < 0.10$), and 10 populations classified as showing clear signs of hybridization (i.e., $0.10 \leq Q_{IT} \leq 0.90$) (Fig. 1d). The genetic substructure within the two lineages was strongly discordant with the spatial distribution of the green-and-black phenotype (Fig. 1d). For example, there were two geographic regions with particularly exaggerated coloration within the IT lineage. One region is located near Rome (e.g., populations FU, LC, RO, FO, SMA) and another region near Pisa (e.g., CR, QC, CA, VI) (Fig. 2c,d), but these regions do not cluster

together genetically (Fig. 1d). Our population genetic analysis also confirms the extensive introgression of the green-and-black phenotype into the SA lineage (Fig. 1d).

Discordance between genetic and phenotypic patterns of variation across the landscape was statistically supported by a multiple matrix regression with randomization (MMRR) on the 43 populations belonging to the IT lineage. Genetic differentiation did not contribute significantly to the phenotypic distance between populations (β_G = -0.17, P = 0.10), while both climatic (β_C = 0.32, P < 0.001) and geographic (β_{Geo} = 0.23, P = 0.001) distance played significant roles. The lack of a relationship between genetic and phenotypic variation allowed us to proceed with spatial modelling of phenotypic variation within the IT lineage in analyses that included populations without genetic data.

Climate explains male color ornamentation within the IT lineage

We first analyzed the data for the IT lineage as this is where the green-and-black phenotype originated (Yang et al. 2018). The green-and-black phenotype showed a linear spatial trend within the IT lineage, with most intense greenness and blackness in the south-west of the lineage's distribution ($F_{2,55}$ = 17.17, P > 0.001; Fig. 2c,d; Fig. S4). The remainder of the analyses therefore proceeded on the detrended data. Forward selection returned four statistically significant dbMEMs (Figs. S5 and S6), which describe the spatial variation in phenotype from broad to very fine scales (e.g., compare MEM2 and MEM8; Fig. S6) The RDA model with these dbMEMs explained 32.5 % of the total variance in green-and-black coloration ($F_{4,53}$ = 7.83; P < 0.001) and returned one statistically significant canonical axis (RDA1: $F_{1,55}$ = 31.65, P < 0.001; RDA2: $F_{1,55}$ = 0.87, P = 0.92; Fig 3a).

Linear regression models, using the first canonical axis scores as the response variable, showed that the spatial variation in phenotype was significantly related to climate PC1 but not PC2 (Table 1), with green-and-black phenotypes being more common in areas that are hot and dry (Fig. 2; Fig. 3a). Partial RDAs and variance partitioning demonstrated that the unique fractions explained by climate, dbMEMs, and the linear trend were all statistically significant (Table S3). Overall, climate explained 40.2% of the variation in green-and-black phenotype across the landscape (Fig. 3a). Most of this variation (34.7%) was spatially structured and mostly accounted for by the linear trend (Fig. 3a), which reflects latitudinal and longitudinal collinearity with climate (Fig 2). The remaining 5.5% of the variation explained uniquely by climate represent climate-phenotype associations on a finer scale than captured by the global linear trend and dbMEMs. The spatial structure captured by the dbMEMs and the linear trend accounted for an additional 25.9% of the variation in the green-and-black phenotype, resulting in 36.6% of variation left unexplained by any of the three variables (Fig. 3a).

Analyses of greenness and blackness separately corroborated that both colors are generally exaggerated in hot and dry climates, but the effects are substantially stronger for greenness than for blackness (all analyses on detrended data; Table 2; Fig. 2e). Greenness was also marginally affected by PC2 (Table 2). Allowing for spatially varying coefficients suggested that the effect of PC1 was consistent across the distribution of the IT lineage, but PC2 showed some evidence for spatially varying coefficients (Figure S7; Table S4). For blackness, the model suggested that the impact of PC1 also varied across the landscape (Figure S8; Table S4).

To further confirm that genetic relatedness did not bias these results, we reran the dbMEM and variance partitioning analyses on the 43 populations for which we had genetic data, including genetic distance as an additional explanatory variable in partial RDAs (see Supplementary

Results). The results confirmed that climate accounted for >40% of the phenotypic variation, of which about 5% was unique to climate (Supplementary Results Table 3 and Fig. 5). Consistent with the MMRR analysis, genetic distance alone was a rather poor predictor of spatial variation in color ornamentation within the IT lineage (for full details, see Supplementary Results).

Climate explains introgression of male color ornamentation

Next, we tested if climate also explains the introgression of the green-and-black phenotype. To this end, we first analyzed the distribution of greenness and blackness for populations that were genetically assigned to the Southern Alps lineage ($Q_{SA} > 0.90$). In this lineage, the green coloration follows closely genetic introgression (Yang et al. 2018), and introgressed populations also exhibit more extensive black coloration (While et al. 2015; Yang et al. 2018).

The introgression of the green-and-black phenotype into the SA lineage showed a strong linear trend ($F_{2,34} = 12.08$, $P < 0.001$; Fig. S9), with a decline in color ornamentation towards the west and north (Fig. 2c,d). The dbMEM analyses for the SA lineage therefore proceeded on the detrended data. Forward selection returned four statistically significant dbMEMs (Fig S10 and S11), which describe the spatial variation in phenotype from broad to very fine scales (e.g., compare MEM2 and MEM10; Fig. S10) The overall model explained 34.9% of the total variation in green-and-black coloration ($F_{4,32} = 5.83$; $P < 0.001$), and returned one statistically significant canonical axis (RDA1: $F_{1,34} = 19.00$; $P < 0.001$; RDA2: $F_{1,34} = 5.77$, $P = 0.12$; Fig. 3b).

Regressing the fitted scores of the first canonical axis revealed that the spatially structured variation in green-and-black phenotype is primarily related to PC2 (Table 3; Fig. 2e), with the green-and-black phenotype being more common in environments characterized by consistently warm climates with wet winters and dry summers (i.e., coastal regions; Fig. 2; Fig. 3a). Partial

RDAs and variance partitioning demonstrated that climate explained 13.2% of the phenotypic variation, the large majority (12.1%) of which was structured by the dbMEM and linear trend (Fig. 3b). The unique fraction (1.1%) explained by climate was not statistically significant (Table S5). Spatial structure and the linear trend accounted for an additional 49.4 % of the phenotypic variation, leaving 37.9% of the variation unexplained (Fig. 3b).

Corroborating the redundancy analysis, univariate regression models with climatic predictors and dbMEMs explained 60% of the variation in greenness, and greenness was significantly related to climatic PC2, but not PC1 (Table 4; Fig. 2). Allowing spatially variable coefficients revealed that the impact of PC2 on greenness was strongest at intermediate distances from the zone of secondary contact (Fig. S12; Table S6). This reflects that populations that are on the coast, but far away from the hybrid zone proper, show no evidence of genetic or phenotypic introgression (see Fig. 1d and Fig. 2c). Relative to greenness, blackness was less structured across the landscape, and neither of the climatic predictors reached statistical significance (Table S6).

While the relatively low number of hybrid populations limited inference for the hybrid zone proper (i.e., $0.10 \leq Q_{IT} \geq 0.90$), the data suggested very similar climate-dependences as for the IT and SA lineage. The green-and-black phenotype showed a linear trend ($F_{2,16} = 3.64$, $P = 0.033$), with decreasing intensity towards the north (Fig. 2c,d and Fig. S13), but there was no evidence of additional spatial structure (i.e., the RDA on the detrended data was not significant; $F_{6,12} = 0.95$, $P = 0.52$). We therefore tested for an effect of climatic PC1 and PC2 by running a multiple regression directly on the (standardized) greenness and blackness data. This showed a statistically significant effect of PC1 and a strong trend for PC2 (Pillai's approximate F-test; PC1: $F_{2,15} = 7.91$, $P = 0.004$; PC2: $F_{2,15} = 3.31$, $P = 0.064$; see Fig. 2e). A partial RDA with climate principal components and linear trend revealed that climate accounted for 29.8% of the total

variation in the green-and-black phenotype (Fig. S14). Most of the explained variation (18.4%) was shared between the linear trend and climate, and neither of the two components explained a significant fraction on their own (Table S7). Given the lack of more complex spatial structure, we did not conduct further univariate analyses using dbMEMs for the hybrid populations.

Discussion

The green-and-black color ornamentation in common wall lizards shows a pronounced variation throughout central and northern Italy, including on a small geographic scale. This variation is evident both within the Italian lineage, where the green-and-black phenotype originated (Yang et al. 2018), as well as across a zone of secondary contact with extensive introgression of the color ornaments. Within lineages, geographic variation in coloration does not reflect genetic differentiation, with steep clines of black and green coloration across populations with extensive gene flow (e.g., eastwards from Rome towards the Apennine mountains).

The striking geographic variation in coloration is difficult to explain unless it is maintained by strong spatial variation in selection (color expression shows limited direct environmental effects; see Introduction). While many un-measured environmental factors will vary across the landscape, our analyses are consistent with climate being a major source of this selection. Firstly, within the Italian lineage, green-and-black coloration was strongly associated with hot and dry climate. Secondly, a consistently warm climate with dry summers appear to promote introgression of color ornamentation into the distantly related Southern Alps lineage. That the best climatic predictor differed between the Italian lineage and for phenotypic introgression into the Southern Alps lineage reflects the climatic variation across the sampling region, and that introgression is ongoing (see below). In fact, the results are remarkably concordant as they establish that male

color ornamentation – and in particular greenness – is most exaggerated in dry and hot Mediterranean summer climates (compare Fig. 2a-d with the climate types in Fig S1). This climate allows a long annual activity period, with consistent and high daily opportunities for activity during the main activity and reproductive season (i.e., spring and summer). In contrast, lizards express the ancestral phenotype at high elevation, which are generally characterized by hibernation during winter, a shorter activity season, and cool and unreliable thermal conditions during spring and summer.

More pronounced sexual ornamentation in environments with a prolonged reproductive season and reliable conditions for lizard activity is consistent with theoretical models of sexual selection (reviewed in Shuster and Wade 2003; Garcia-Roa et al. 2020). Sexual selection in wall lizards is predominantly a result of intense competition between males, who defend territories and females, and occasionally venture into the territories of other males in search of mating opportunities (Edsman 1990; Heathcote et al. 2016; MacGregor et al. 2017a; Abalos et al. 2020). An extended and poorly synchronized breeding season can result in a sustained presence of receptive females, which allows dominant males to acquire a disproportionate mating success and result in stronger sexual selection compared to a shorter and more synchronous breeding season (Emlen and Oring 1977; Shuster and Wade 2003). This phenomenon is exemplified by a long-term study of sand lizards (*Lacerta agilis*) at the species' climatic extreme in Sweden. Warmer years prolonged the mating period, allowing males to mate with more females and resulting in more intense competition for fertilizations (Olsson et al. 2011a; Olsson et al. 2011b). Female wall lizards do not choose males based on their coloration or morphology (e.g., Heathcote et al. 2016; MacGregor et al. 2017a; Abalos et al. 2020), and it therefore appears unlikely that differences in female choosiness contribute to the geographic variation in male coloration. As population genetic

differentiation explained very little of the geographic variation in coloration, phenotypic divergence in male ornamentation *per se* likely has a weak effect on the evolution of reproductive isolation (Servedio and Boughman 2017; but see Yang et al. 2020 for how ornamentation can mediate the extent of introgression). More importantly in this context is that female wall lizards in cool climates lay fewer clutches and invest more in the first clutch (MacGregor et al. 2017b), and that breeding may be initiated more rapidly following hibernation (Bonnet et al. 1998). As a result, receptive females will tend to be clustered in time (at least within a given microhabitat), limiting the number of females a male can gain access to (Emlen and Oring 1977; Shuster and Wade 2003). Further field studies of the distribution of males and receptive females and direct estimates of reproductive success (from paternity; Olsson et al. 2019) could substantiate this explanation for the geographic mosaic of color ornamentation in common wall lizards and other species (see Shuster and Wade 2003 for discussion). We suggest that climatic effects on male activity and the distribution of receptive females is wide-spread in ectotherms, and contribute to geographic mosaics in the strength of sexual selection in both vertebrates and invertebrates (Gosden and Svensson 2008; Snell-Rood and Badyaev 2008; Punzalan et al. 2010; Miller and Svensson 2014).

While climatic effects on the strength of sexual selection is a plausible explanation for the geographic variation in male ornamentation in common wall lizards, there are at least four alternative and complementary reasons why selection may maintain population differentiation in ornamentation across climatic regimes. First, green and black colors may be less effective as signals in cool and wet climates, for example, because of variation in light conditions and background matching (Endler 1992; McLean et al. 2014; Perez i de Lanuza and Font 2016). Although such differences can be subtle, and cannot be ruled out, the explanation appears unlikely given that the typical habitats (e.g., dry stone walls, open forest) are similar across climatic regimes

and for the two lineages. However, human activities have changed the Italian landscape over millennia, and some of the phenotypic variation observed today may reflect regional differences in habitat or other environmental factors that were pronounced in the past. Second, the green-and-black phenotype could be associated with significant fitness costs and benefits beyond communication to conspecifics (or arise as a side-effect of communication). For example, variation in predation risk can vary with climate (Vucic-Pestic et al. 2011; Dell et al. 2014), and therefore impose a fitness cost on bright animals irrespective of sex (Martin and Lopez 2001; Marshall et al. 2015). We cannot exclude this possibility but have no reason to expect such large, and geographically variable, differences in predation risk for conspicuous animals. Third, colors could have biological functions other than communication, such as thermoregulation. Dark body coloration can be favored in cool climates if it helps the animals heat faster and maintain higher equilibrium temperatures (Clusella Trullas et al. 2007). This prediction is opposite to the distribution of ventral blackness in common wall lizards, since it was most pronounced in hot and dry climates. However, it is notable that blackness showed a weaker and less consistent association with climate than dorsal greenness. Thus, although greenness and blackness are correlated at both individual and population level (including during introgression), selection on blackness may be relatively weaker or more variable across climatic regimes. Fourth, the green-and-black phenotype could have an underlying genetic basis that affects other (i.e., non-coloration) traits that make lizards poorly adapted to cool climate. Indeed, there is extensive evidence from mammals and birds that melanization could be inherently pleiotropic, in particular with respect to physiology (San-Jose and Roulin 2018). The same applies to carotenoids and pterins (e.g., Svensson and Wong 2011), which may be involved in the green dorsal coloration. To evaluate this hypothesis, it will

be necessary to establish how coloration is genetically, developmentally and functionally integrated with other traits.

Our study identifies climate as a very important factor in the evolution of sexual coloration. However, there are undoubtedly other traits (e.g. food availability, habitat quality) that vary across the landscape and in turn mediate a range of factors (e.g., variation in population density, reproductive output, sex ratios) that are known to promote or relax sexual selection. Furthermore, selection is of course not the sole reason that animal coloration varies across the landscape. The poor concordance between genetic and phenotypic differentiation suggests that historical or contemporary restrictions on gene flow have little effect on the geographic distribution of male color ornamentation. However, several lines of evidence suggest that the spread of the phenotype is ongoing and hence not at an equilibrium. Recent genetic analyses have revealed that the green-and-black phenotype in common wall lizards is rather recent, and it may have originated in the south-west of the current distribution of the Italian lineage (Yang et al. 2018; Yang et al. 2020), which is where the characters are most exaggerated. Thus, the limited expression of the characters at the northern limit of the Italian lineage, on the Po plain, is consistent with an ongoing spread of coloration from the south. Whether or not that is the case, an ongoing introgressive spread is strongly supported by the very strong decline in the introgression of green dorsal coloration with increasing distance from the hybrid zone. In fact, the analyses suggest that the green-and-black phenotype is absent from regions where it should be under positive selection (in particular along the coast further west). We therefore conclude that this exaggerated body coloration is likely to continue its introgression where the climate allows high lizard activity and long reproductive seasons, further contributing to the mosaic distribution of coloration in this species.

Acknowledgements

We are grateful to the many field assistants, and to Nathalie Feiner for discussion and help with the preparation of figures. The associate editor and two anonymous reviewers provided helpful comments on the manuscript. The Ministry of Education, University and Research (MIUR) provided all the authorizations for the study, 2012-2013: Aut. Prot. PNM-0009344; 2014-2015: Aut. Prot. PNM-0011379; 2016-2018: Aut. Prot. PNM-0002154. This work was funded by the Royal Society of London, the National Geographic Society, the British Ecological Society, the Swedish Research Council, and a Wallenberg Academy Fellowship from the Knut and Alice Wallenberg Foundations (all to TU).

Statement of Authorship

M.R.M, G.M.W, and T.U. conceived and designed the study; MRM, GMW, WY, RS, MZ, SS, DS and TU contributed to field data collection; M.R.M. and W.Y. performed the molecular lab work; M.R.M. and T.U. analyzed the data with input from G.M.W., W.Y. and C.P.B. T.U. wrote the first draft, and M.R.M., G.M.W., C.P.B. and T.U reviewed and edited the manuscript.

Data code and accessibility

Data available at Dryad Digital Repository, DOI: https://doi.org/10.5061/dryad.s1rn8pk7c, and GenBank, accession number: PRJNA486080.

Literature Cited

Abalos, J., G. Pérez i de Lanuza, A. Bartolomé, O. Liehrmann, H. Laakkonen, F. Aubret, T. Uller et al. 2020. No evidence for differential sociosexual behavior and space use in the

color morphs of the European common wall lizard (*Podarcis muralis*). Ecology and Evolution 10:10986-11005.

Adolph, S. C. and W. P. Porter. 1993. Temperature, activity, and lizard life histories. American Naturalist 142:273-295.

Alexander, D. H., J. Novembre, and K. Lange. 2009. Fast model-based estimation of ancestry in unrelated individuals. Genome Research 19:1655-1664.

Andrade, P., C. Pinho, G. Pérez i de Lanuza, S. Afonso, I. Bunikis, M. A. Carretero, N. Feiner, P. Marsik, F. Paupério, D. Salvi, L. Soler. et al. 2019. Regulatory changes in pterin and carotenoid genes underlie balanced color polymorphisms in the wall lizard. Proceedings of the National Academy of Sciences of the USA 116:5633-5642.

Angilletta, M. J. 2009. Thermal adaptation. Oxford University Press, New York, NY.

Arnold, M. L. 2016. Divergence with genetic exchange. Oxford University Press, New York, NY.

Barton, N. H. and G. M. Hewitt. 1989. Adaptation, speciation and hybrid zones. Nature 341:497-503.

Beck, Hylke E.; Zimmermann, Niklaus E.; McVicar, Tim R.; Vergopolan, Noemi; Berg, Alexis; Wood, Eric F. 2018. Present and future Köppen-Geiger climate classification maps at 1-km resolution. Scientific Data. **5**: 180214.

Blanchet, F. G., P. Legendre, and D. Borcard. 2008. Modelling directional spatial processes in ecological data. Ecological Modelling 215:325-336.

Bonnet, X., D. Bradshaw, and R. Shine. 1998. Capital versus income breeding: an ectothermic perspective. Oikos 83:333-342.

Borcard, D., F. Gillet, and P. Legendre. 2018. Numerical ecology with R. Springer Verlag.

Catchen, J., P. A. Hohenlohe, S. Bassham, A. Amores, and W. A. Cresko. 2013. Stacks: An analysis tool set for population genomics. Molecular Ecology 22:3124-3140.

Chang, C. C., C. C. Chow, L. C. Tellier, S. Vattikuti, S. M. Purcell and J. J. Lee 2015. Second-generation PLINK: rising to the challenge of larger and richer datasets. Gigascience 4:s13742-015.

Clusella Trullas, S., J. H. van Wyk, and J. R. Spotila. 2007. Thermal melanism in ectotherms. Journal of Thermal Biology 32:235-245.

Cornwallis, C. K. and T. Uller. 2010. Towards an evolutionary ecology of sexual traits. Trends in Ecology and Evolution 25:145-152.

Cyrén, O. 1924. Klima und Eidechsenverbreitung. Eine Studie der geographischen Variation und Entwicklung einiger Lacerten, insbesondere unter Berücksichtigung der klimatischen Faktoren. Medd. Göteborg Km., Zool. Avd 29:1-82.

Dell, A. I., S. Pawar, and V. M. Savage. 2014. Temperature dependence of trophic interactions are driven by asymmetry of species responses and foraging strategy. Journal of Animal Ecology 83:70-84.

Dray, S. and A. B. Dufour. 2007. The ade4 package: implementing the duality diagram for ecologists. Journal of Statistical Software 22:1-20.

Dray, S., P. Legendre, and P. R. Peres-Neto. 2006. Spatial modelling: a comprehensive framework for principal coordinate analysis of neighbour matrices (PCNM). Ecological Modelling 196:483-493.

Dray, S., R. Pélissier, P. Couteron, M. J. Fortin, P. Legendre, P. R. Peres-Neto, E. Bellier, R. Bivand, F. G. Blanchet, M. De Caceres, A. B. Dufour, E. Heegaard, T. Jombart, F.

Munoz, J. Oksanen, J. Thioulouse, and H. H. Wagner. 2012. Community ecology in the age of multivariate multiscale spatial analysis. Ecological Monographs 82:257-275.

Edsman L. 1990. Territoriality and competition in wall lizards. PhD thesis, Department of Zoology, University of Stockholm

Eimer, T. 1881. Untersuchungen über das Variiren der Mauereidechse: ein Beitrag zur Theorie von der Entwicklung aus constitutionellen Ursachen, sowie zum Darwinismus. Nicolaische Verlag Buchhandlung, Berlin.

Emlen, S. T. and L. W. Oring. 1977. Ecology, sexual selection, and evolution of mating systems. Science 197:215-223.

Endler, J. A. 1992. Signals, signal conditios, and the direction of evolution. American Naturalist 139: S125-S153.

Evans, S. R. and L. Gustafsson. 2017. Climate change upends selection on ornamentation in a wild bird. Nature Ecology and Evolution 1:0039.

Fan, Z., P. Silva, I. Gronau, S. Wang, A. S. Armero, R. M. Schweizer, O. Ramirez, J. Pollinger, M. Galaverni, D. O. Del-Vecchyo, L. Du, W. Zhang, Z. Zhang, J. Xing, C. Vilà, T. Marques-Bonet, R. Godinho, B. Yue, and R. K. Wayne. 2016. Worldwide patterns of genomic variation and admixture in gray wolves. Genome Research 26:163-173.

Fick, S. E. 2017. WorldClim 2: new 1-km spatial resolution climate surfaces for global land areas. International Journal of Climatology 4315:4302-4315.

Fortin, M.-J. and M. Dale. 2005. Spatial Analysis: A Guide for Ecologists. Cambridge University Press.

Garcia-Roa, R., V. Chirinos, and P. Carazo. 2019. The ecology of sexual conflict: Temperature variation in the social environment can drastically modulate male harm to females. Functional Ecology 33:681-692.

Garcia-Roa, R., F. Garcia-Gonzaléz, D. W. A. Noble, and P. Carazo. 2020. Temperature as a modulator of sexual selection and sexual conflict. Biological Reviews 95:1607-1629.

Gosden, T. P. and E. I. Svensson. 2008. Spatial and temporal dynamics in a sexual selection mosaic. Evolution 62:845-856.

Heathcote, R. J. P., G. M. While, H. E. A. Macgregor, J. Sciberras, C. Leroy, P. D. Ettorre, and T. Uller. 2016. Male behaviour drives assortative reproduction during the initial stage of secondary contact. Journal of Evolutionary Biology 29:1003-1015.

Hedrick, P. W. 2013. Adaptive introgression in animals: examples and comparison to new mutation and standing variation as sources of adaptive variation. Molecular Ecology 22:4606-4618.

Legendre, P., and M.J. Andersson 1999. Distance-based redundancy analysis: Testing multispecies responses in multifactorial ecological experiments. Ecological Monographs 69:1–24.

Legendre, P. and L. Legendre. 2012. Numerical Ecology. Elsevier, Amsterdam, the Netherlands.

Macgregor, H. E. A., G. M. While, J. Barrett, P. Guillem, P. Carazo, S. Michaelides and T. Uller. 2017a. Experimental contact zones reveal causes and targets of sexual selection in hybridizing lizards. Functional Ecology 31:742-752.

MacGregor, H. E. A., G. M. While, and T. Uller. 2017b. Comparison of reproductive investment in native and non-native populations of common wall lizards reveals sex differences in adaptive potential. Oikos 126:1564-1574.

Macías-Ordóñez, R., G. Machado, and R. H. Macedo. 2013. Macroecology of Sexual Selection: Large-Scale Influence of Climate on Sexually Selected Traits. Pp. 1-32 *in* R. H. Macedo, and G. Machado, eds. Sexual Selection. Academic Press, San Diego.

Marshall, K. L. A., K. E. Philpot, and M. Stevens. 2015. Conspicuous male coloration impairs survival against avian predators in Aegean wall lizards, *Podarcis erhardii*. Ecology and Evolution 5:4115-4131.

Martín, J. and P. López. 2001. Risk of predation may explain the absence of nuptial coloration in the wall lizard *Podarcis muralis.* Evolutionary Ecology Research 3:889-898.

McLean, C. A., A. Moussalli, and D. Stuart-Fox. 2014. Local adaptation and divergence in colour signal conspicuousness between monomorphic and polymorphic lineages in a lizard. Journal of Evolutionary Biology 27:2654-2664.

McLean, C. A. and D. Stuart-Fox. 2014. Geographic variation in animal colour polymorphisms and its role in speciation. Biological Reviews 89:860-873.

McLean, C. A., D. Stuart-Fox, and A. Moussalli. 2015. Environment, but not genetic divergence, influences geographic variation in colour morph frequencies in a lizard. BMC Evolutionary Biology 15:156.

Miller, C. W. and E. I. Svensson. 2014. Sexual selection in complex environments. Annual Review of Entomology 59:427-445.

Moore, M. P., C. Lis, I. Gherghel, and R. A. Martin. 2019. Temperature shapes the costs, benefits and geographic diversification of sexual coloration in a dragonfly. Ecology Letters 22:437-446.

Murakami, D. 2020. spmoran: Moran Eigenvector-Based Scalable Spatial Additive Mixed Modeling. R package version 0.2.0-2.https://CRAN.R-project.org/package=spmoran

Murakami, D. and D. A. Griffith. 2019. Eigenvector Spatial Filtering for Large Data Sets: Fixed and Random Effects Approaches. Geographical Analysis 51:23-49.

Murakami, D., T. Yoshida, and H. Seya. 2017. A Moran coefficient-based mixed effects approach to investigate spatially varying relationships. Spatial Statistics 19:68-89.

Oksanen, J., R. Kindt, P. Legendre, D. McGlinn, P. R. Minchin, R. B. O'Hara, G. L. Simpson, P. Solymos, M. H. H. Stevens, E. Szoecs, H. Wagner. 2019. Vegan: Community Ecology Package. R package version 2.5-6. Package 'vegan'. https://CRAN.R-project.org/package=vegan.

Olsson, M., T. Schwartz, E. Wapstra, T. Uller, B. Ujvari, T. Madsen, and R. Shine. 2011a. Climate change, multiple paterniy and offspring survival in lizards. Evolution 65:3323-3326.

Olsson, M., T. S. Schwartz, E. Wapstra, and R. Shine. 2019. How accurately do behavioural observations predict reproductive success in free-ranging lizards? Biology Letters 15: 20190030.

Olsson, M., E. Wapstra, T. Schwartz, T. Madsen, B. Ujvari, and T. Uller. 2011b. In hot pursuit: Fluctuating mating system and sexual selection in sand lizards. Evolution 65:574-583.

Orteu, A. and C. D. Jiggins. 2020. The genomics of coloration provides insights into adaptive evolution. Nature Reviews Genetics 21:461-475.

Peres-Neto, A. P. R., P. Legendre, S. Dray, and D. Borcard. 2006. Variation partitioning of species data matrices. Ecology 87:2614-2625.

Perez i de Lanuza, G. and E. Font. 2016. The evolution of colour pattern complexity: selection for conspicuousness favours contrasting within-body colour combinations in lizards. Journal of Evolutionary Biology 29:942-951.

Pérez i de Lanuza, G., E. Font, and J. L. Monterde. 2013. Using visual modelling to study the evolution of lizard coloration: Sexual selection drives the evolution of sexual dichromatism in lacertids. Journal of Evolutionary Biology 26:1826-1835.

Punzalan, D., F. H. Rodd, and L. Rowe. 2010. Temporally variable multivariate sexual selection on sexually dimorphic traits in a wild insect population. American Naturalist 175:401-414.

Rosenthal, M. F. and D. O. Elias. 2019. Nonlinear changes in selection on a mating display across a continuous thermal gradient. Proceedings of the Royal Society B 286:20191450.

Ruiz Miñano, M., G. M. While, W. Yang, C. P. Burridge, R. Sacchi, M. Zuffi, S. Scali, D. Salvi and T. Uller. 2021. Data from: Climate shapes the geographic distribution and introgressive spread of colour ornamentation in common wall lizards. American Naturalist, Dryad Digital Repository, https://doi.org/10.5061/dryad.s1rn8pk7c

San-Jose, L. M. and A. Roulin. 2018. Toward understanding the repeated occurrence of associations between melanin-based coloration and multiple phenotypes. American Naturalist 192:111-130.

Schulte, U., A. Hochkirch, S. Loetters, D. Roedder, S. Schweiger, T. Weimann, and M. Veith. 2012. Cryptic niche conservatism among evolutionary lineages of an invasive lizard. Global Ecology and Biogeography 21:198-211.

Servedio, M. R. and J. W: Boughman. 2017. The role of sexual selection in local adaptation and speciation. Annual Reviews of Ecology, Evolution and Systematics 48:85-109.

Shuster, S. M. and M. Wade. 2003. Mating systems and strategies. Princeton University Press, Princeton, NJ.

Sinervo, B., F. Méndez-de-la-Cruz, D. B. Miles, B. Heulin, E. Bastiaans, M. V. S. Cruz, R. Lara-Resendiz, N. Martínez-Méndez, M. L. Calderón-Espinosa, R. N. Meza-Lázaro, H. Gadsden, L. J. Avila, M. Morando, I. J. De La Riva, P. V. Sepúlveda, C. F. D. Rocha, N. Ibargüengoytía, C. A. Puntriano, M. Massot, V. Lepetz, T. A. Oksanen, D. G. Chappie, A. M. Bauer, W. R. Branch, J. Clobert, and J. W. Sites. 2010. Erosion of lizard diversity by climate change and altered thermal niches. Science 328:894-899.

Snell-Rood, E. and A. Badyaev. 2008. Ecological gradient of sexual selection: elevation and song elaboration in finches. Oecologia 157:545-551.

Svensson, E. I. 2019. Eco-evolutionary dynamics of sexual selection and sexual conflict. Functional Ecology 33:60-72.

Svensson, P. A. and B. B. M. Wong. 2011. Carotenoid-based signals in behavioural ecology: a review. Behaviour 148:131-189.

Uy, J. A. C. and A. C. Stein. 2007. Variable visual habitats may influence the spread of colourful plumage across an avian hybrid zone. Journal of Evolutionary Biology 20:1847-1858.

Vucic-Pestic, O., R. B. Ehnes, B. C. Rall, and U. Brose. 2011. Warming up the system: Higher predator feeding rates but lower energetic efficiencies. Global Change Biology 17:1301-1310.

Wang, I. J. 2013. Examining the full effects of landscape heterogeneity on spatial genetic variation: A multiple matrix regression approach for quantifying geographic and ecological isolation. Evolution 67:3403-3411.

While, G. M., S. Michaelides, R. J. P. Heathcote, H. E. A. MacGregor, N. Zajac, J. Beninde, P. Carazo, G. Pérez i de Lanuza, R. Sacchi, M. A. L. Zuffi, T. Horváthová, B. Fresnillo, U.

Schulte, M. Veith, A. Hochkirch, and T. Uller. 2015. Sexual selection drives asymmetric introgression in wall lizards. Ecology Letters 18:1366-1375.

Yang, W., N. Feiner, H. Laakkonen, R. Sacchi, M. A. L. Zuffi, S. Scali, G. M. While, and T. Uller. 2020. Spatial variation in gene flow across a hybrid zone reveals causes of reproductive isolation and asymmetric introgression in wall lizards. Evolution:1-12.

Yang, W., G. M. While, H. Laakkonen, R. Sacchi, M. A. L. Zuffi, S. Scali, and D. Salvi. 2018. Genomic evidence for asymmetric introgression by sexual selection in the common wall lizard. Molecular Ecology:4213-4224.

Tables

Table 1. Linear regression of the fitted scores for the first canonical axis (RDA1) on the two climatic principal components in the Italian lineage.

Coefficients	Estimate ± SE	t-value	P-value
Intercept	0.066 ± 0.040	1.63	0.11
PC1	0.271 ± 0.100	2.70	0.009
PC2	-0.008 ± 0.108	-0.07	0.95

Overall model: $F_{2,55} = 4.11$, $P = 0.02$; Adjusted $R^2 = 0.10$; Residual error: 0.219. Negative scores for RDA1 represents populations with more exaggerated colors.

Table 2. Spatial random effects regression models on standardized greenness and standardized blackness scores for the Italian lineage. The two climatic principal components were entered as explanatory variables.

	Greenness			Blackness		
Coefficients	Estimate ± SE	t-value	P-value	Estimate ± SE	t-value	P-value
Intercept	-0.320 ± 0.093	-3.45	0.001	-0.190 ± 0.119	-1.59	0.12
PC1	-1.118 ± 0.268	-4.17	0.001	-0.751 ± 0.344	-2.18	0.03
PC2	0.591 ± 0.308	1.92	0.06	0.091 ± 0.389	0.23	0.82

Greenness model: Standard error of the estimated spatial process = 0.47; Residual standard error = 0.43; Scaled Moran's coefficient = 0.16; Adjusted R^2 = 0.61

Blackness model: Standard error of the estimated spatial process = 0.57; Residual standard error = 0.56; Scaled Moran's coefficient = 0.22; Adjusted R^2 = 0.52

Table 3. Linear regression of the fitted scores for the first canonical axis (RDA1) on the two climatic principal components in the Southern Alps lineage.

Coefficients	Estimate ± SE	t-value	P-value
Intercept	-0.073 ± 0.041	-1.76	0.08
PC1	0.130 ± 0.075	1.73	0.09
PC2	-0.377 ± 0.111	-3.40	0.002

Overall model: $F_{2,34} = 6.34$, P = 0.005; Adjusted $R^2 = 0.23$. Residual error: 0.212. Positive scores for RDA1 represents populations with more exaggerated colors.

Table 4. Spatial random effects regression models on (left) standardized greenness and (right) standardized blackness scores for the Southern Alps lineage. The two climatic principal components were entered as explanatory variables.

	Greenness			Blackness		
Coefficients	Estimate ± SE	t-value	P-value	Estimate ± SE	t-value	P-value
Intercept	-0.107 ± 0.093	-1.15	0.25	-0.001 ± 0.151	-0.06	0.95
PC1	-0.119 ± 0.187	-0.63	0.53	-0.125 ± 0.303	-0.41	0.68
PC2	-0.987 ± 0.350	-2.82	0.008	-0.246 ± 0.552	-0.45	0.65

Greenness model: Standard error of the estimated spatial process = 0.47; Residual standard error = 0.42; Scaled Moran's coefficient = 0.27; Adjusted R^2 = 0.61

Blackness model: Standard error of the estimated spatial process = 0.71; Residual standard error = 0.70; Scaled Moran's coefficient = 0.16; Adjusted R^2 = 0.13

Figure Legends

Figure 1. (A) A male *P. muralis* from the IT lineage with an exaggerated green-and-black phenotype. (B) A male *P. muralis* from the IT lineage with the ancestral phenotype. (C) Results from a Principal Component Analysis of the individual SNP data, illustrating the separation between the IT and SA lineages, and different degrees of admixture. (D) Results from the ADMIXTURE analysis for K=2-5 illustrate the variation in greenness and blackness within each of the two main lineages (IT and SA; K = 2), and the poor concordance between lizard coloration and genetic structure within both lineages with increasing K (for full results for K= 2-15, see Figure S1). Colors of the ADMIXTURE plot indicate genetic clusters. Color panels above the ADMIXTURE plot represents the intensity of the average dorsal greenness (light green = more intense green dorsal color) and the height of the black bars represents the average proportion of black pigmentation on the chest (ranging from zero to one) for each population. Photo credits: Nathalie Feiner.

Figure 2. Summary of climatic and phenotypic variation in the study area. (A) Climatic PC1, representing a gradient from hot and dry (negative values, red) to cool and wet (positive values, blue). (B) Climatic PC2, represent a gradient from mild, wet winters and warm to hot, dry summers (negative values, red) to cool winters and warm summers with significant precipitation even during the driest month (positive values, blue); (C) Geographic distribution of the average intensity of male green dorsal coloration. Light green represents more intense coloration. (D) Geographic distribution of the average proportion of male black pigmentation on the chest (ranging from zero to one). Black dots in panels C and D represent populations of the Italian (IT) lineage, orange dots

populations of the Southern Alps (SA) lineage, and blue dots the hybrid zone (mixed origin). Interpolation of coloration on the map uses inverse distance weights. (E) Correlations between Greenness and Blackness and the two climatic principal components (PC1 and PC2) for each of the lineages and the hybrid zone proper.

Figure 3. Results from the dbMEM analyses and variance partition of the colouration data for (A) the Italian (IT) lineage, and (B) the Southern Alps (SA) lineage. Top row: RDA triplots with two canonical axes (RDA1 and RDA2). Black circles represent populations, grey vectors represent the dbMEM predictors, and green and black vectors the response variables greenness and blackness, respectively. Middle row: Fitted scores of the first canonical axis of the redundancy analysis (i.e., RDA1 from top panel). Each dot represents a population; the size and color of the dots indicate the fitted score of RDA1, with white dots representing negative, and black dots representing positive, scores. For interpretation on its relationship to greenness and blackness, compare with the plots in the top row (e.g., for the IT lineage in (A), populations represented by large white dots on the map are those with the most intense green-and-black phenotype). Bottom row: Variance partitioning of the coloration data with unique and shared fractions of explained variation. Empty fractions are estimated to have zero variance.

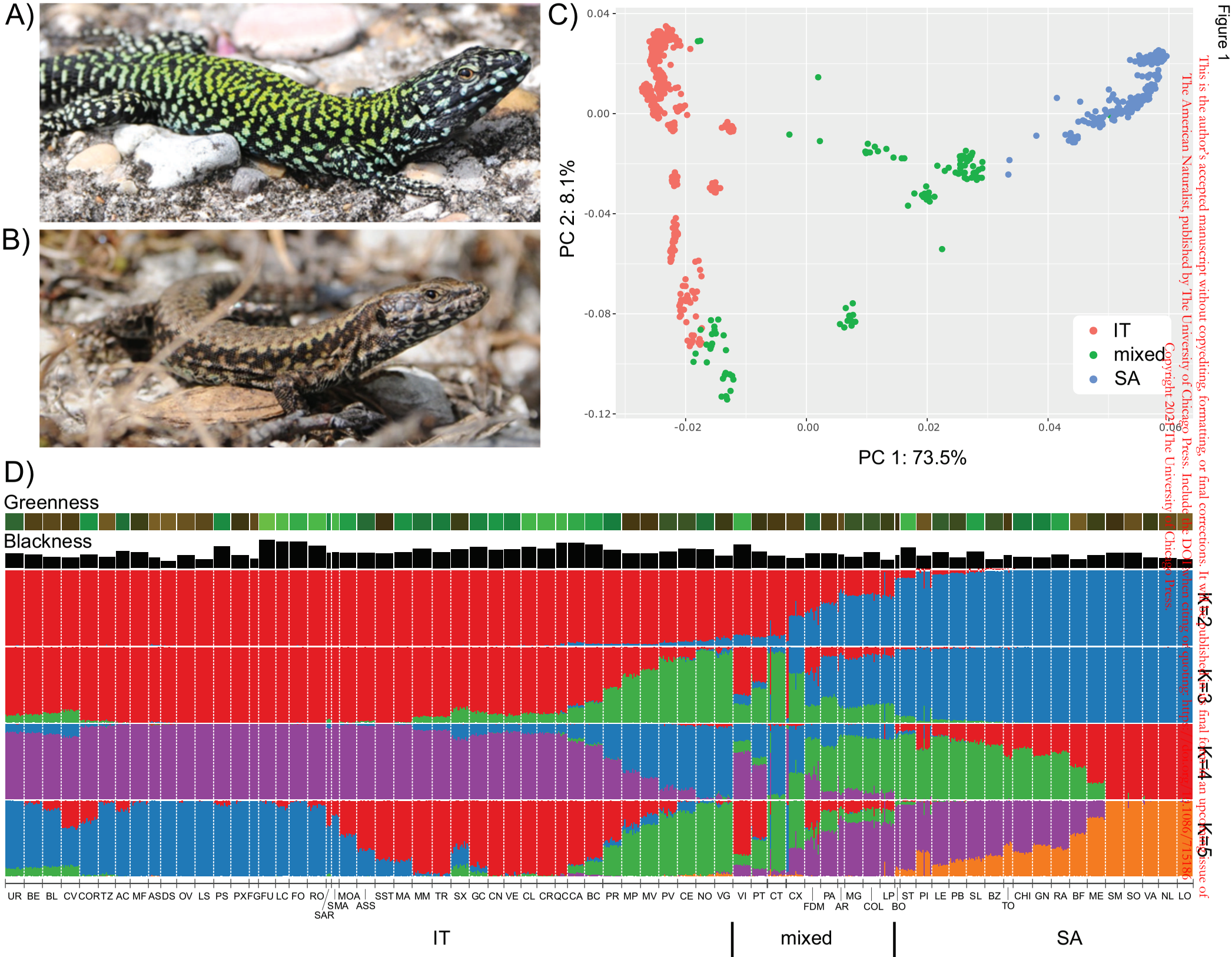

Figure 1

Figure 2

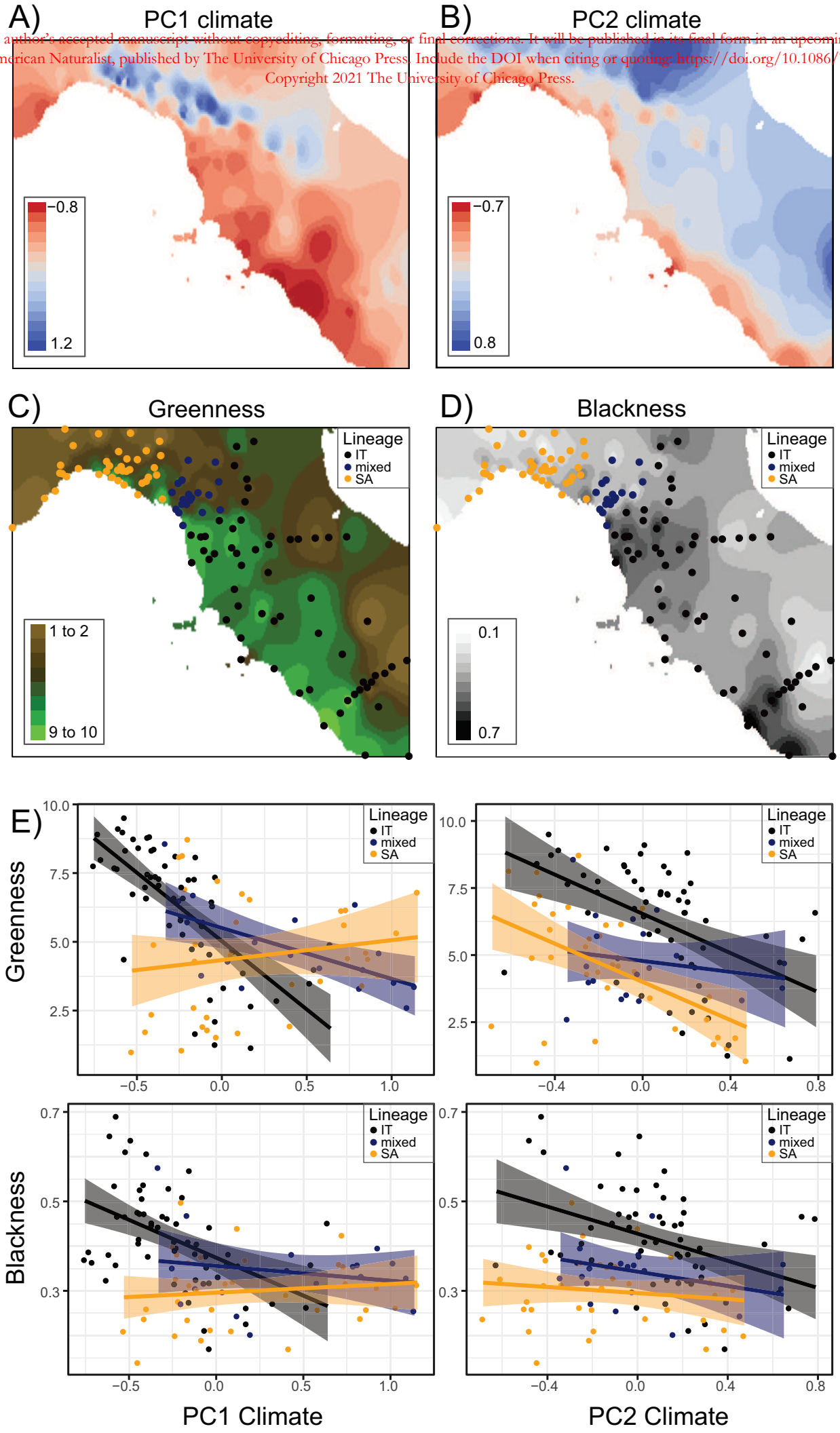

Figure 3

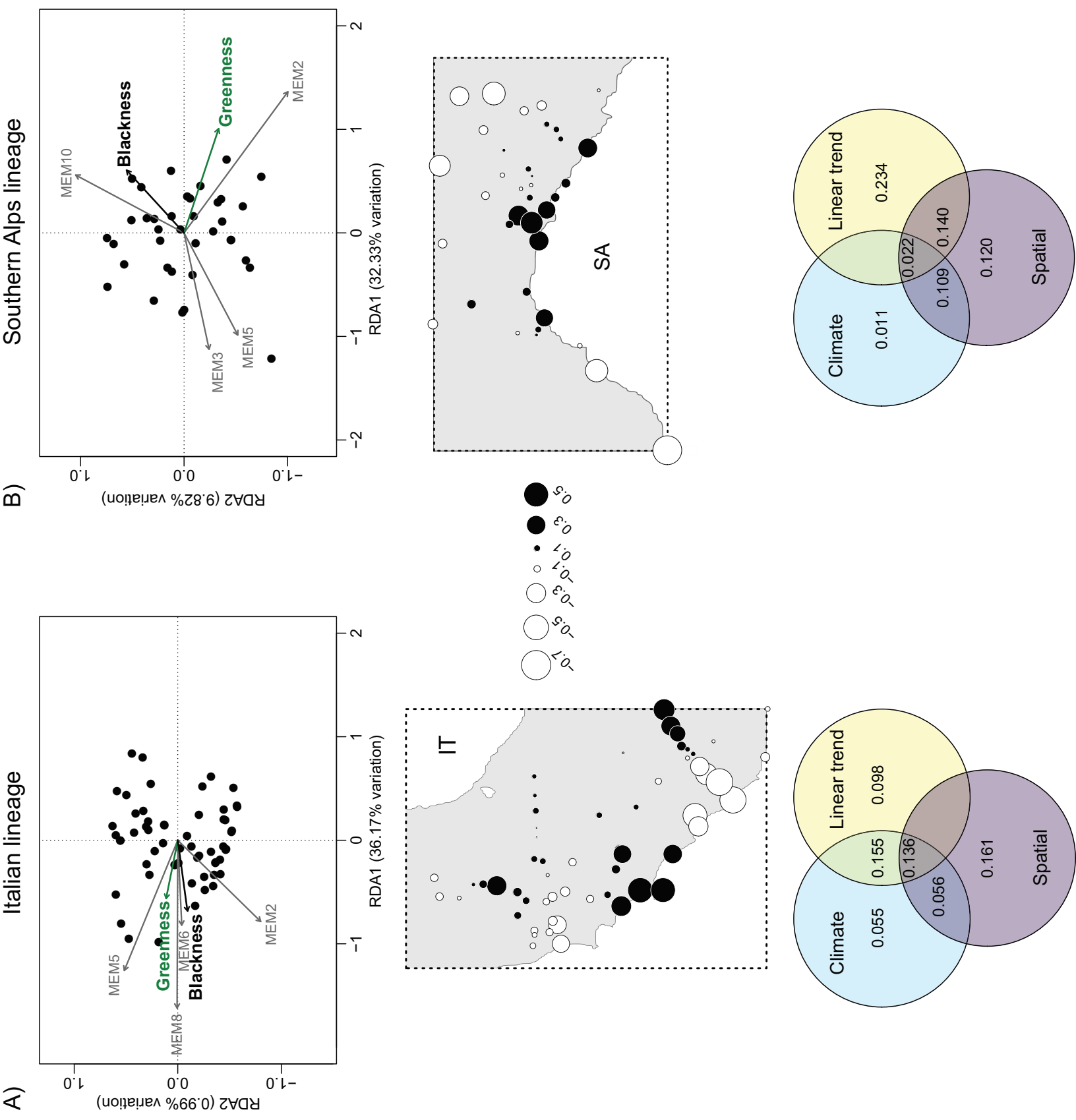

Supplementary Material

Climate shapes the geographic distribution and introgressive spread of colour ornamentation in common wall lizards

Maravillas Ruiz Miñano[1,2], Geoffrey M. While[2], Weizhao Yang[1], Christopher P. Burridge[2], Roberto Sacchi[3], Marco Zuffi[4], Stefano Scali[5], Daniele Salvi[6] & Tobias Uller[1]

1. Department of Biology, Lund University, Sölvegatan 37, 223 62 Lund, Sweden

2. School of Biological Sciences, University of Tasmania, Hobart, Tasmania 7005, Australia

3. Department of Earth and Environmental Sciences, University of Pavia, Viale Taramelli 24, 27100 Pavia, Italy

4. Museum of Natural History, University of Pisa, via Roma 79, 56011 Calci (Pisa), Italy

5. Museum of Natural History, corso Venezia 55, 20121 Milano, Italy

6. Department of Health, Life and Environmental Sciences, University of L'Aquila, Via Vetoio, 67100 Coppito, L'Aquila, Italy

Corresponding author: Tobias Uller, tobias.uller@biol.lu.se

Published in the American Naturalist

This file contains the following sections:

1. Supplementary Results, including accompanying tables and figures
2. Supplementary Tables S1-S7, referred to in the main text
3. Supplementary Figures S1-S14, referred to in the main text

1. Supplementary Results

Climate explains male colour ornamentation within the IT lineage

While the MMRR analysis suggested that genetic differentiation within the IT lineage was a poor predictor of the spatial distribution of the green-and-black phenotype, we repeated the dbMEM analysis on the subset of 43 IT populations for which we had genetic data (Fig. 1.1; all figure numbers refer to the figures at the end of this document unless otherwise specified). This allowed us to include eigenvalues from a principal coordinate analysis (PCoA) on the pairwise F_{ST} as explanatory variable in the partial RDA and variance partitioning (Legendre and Andersson, 1999).

Similar to the results for the 58 populations, the green-and-black phenotype showed a linear spatial trend within the IT lineage ($F_{2,40} = 13.12$, $P > 0.001$; Fig. 1.2). The remainder of the analyses therefore proceeded on the detrended data. Forward selection returned two statistically significant dbMEMs (Figs. 1.3 and 1.4). The RDA model with these dbMEMs explained 36.6 % of the total variance in green-and-black colouration ($F_{2,40} = 13.13$; $P < 0.001$) and returned one statistically significant canonical axis (RDA1: $F_{1,40} = 25.87$, $P < 0.001$; RDA2: $F_{1,40} = 0.39$, $P = 0.63$; Fig 1.5a).

Linear regression models, using the first canonical axis scores as the response variable, showed that the spatial variation in phenotype was borderline significant for both climate PC1 and PC2 (Table 1.1; both were significant at $P < 0.05$ when entered as the sole predictor). Partial RDAs and variance partitioning demonstrated that the unique fractions explained by climate, dbMEMs, and the linear trend were all statistically significant (Table 1.2). The shared and unique fractions explained by the three predictors corresponded well with results for the 58 populations (compare Fig. 1.5 in this supplement with Fig. 3a in the main paper).

Having verified that the results for these 43 populations were similar to results that include all 58 populations, we proceeded to add genetic distance as an explanatory variable. A

PCoA on the pairwise F_{ST} resulted in the retention of three axes for downstream analysis (using the broken stick method). The partial RDA analyses revealed a strong linear dependency between x,y coordinates and this estimate of genetic distance (variance inflaction factor > 40 for both x and y coordinates). Since our main aim was to verify that genetic distance did not confound our estimate of the variation in greenness and blackness explained by climate, we therefore simply dropped the x,y coordinates and run partial RDAs and variance partitioning with climate (PC1 and PC2), spatial structure (dbMEMs), and genetic distance (Axis 1-3). The results revealed qualitatively similar results as the partial RDAs with x.y coordinates, with all three explanatory variables (climate, spatial structure and genetic distance) explaining a unique fraction of phenotypic variation (Table 1.3; Fig. 1.5). For completeness, the variogram for all four explanatory variables (climate, spatial structure, linear trend and genetic distance) is presented in Fig. 1.6. Note that the shared fraction of variance between climate and genetic distance alone is estimated to be zero.

Overall, these analyses confirm that climate explains a substantial (> 40%) amount of variation in the green-and-black phenotype within the IT lineage. Most of this variation is spatially structured. While genetic differentiation may partly account for the linear trend, in particular from south-to-north (see Fig. 1 in the main paper), population genetic differentiation appears to have a rather limited explanatory power for the fine- and medium-scale variation in the expression of colour ornamentation in this lineage of *P. muralis*.

References

Legendre, P., & Andersson, M. J. (1999). Distance-based redundancy analysis: Testing multispecies responses in multifactorial ecological experiments. *Ecological Monographs*, *69*(1), 1–24.

Tables accompanying supplementary results

Table 1.1. Linear regression of the fitted scores for the first canonical axis (RDA1) on the two climatic principal components in the Italian lineage. Full model: $F_{2,40} = 5.09$, $P = 0.01$; Adjusted $R^2 = 0.16$; Residual error: 0.235. Negative scores for RDA1 represents populations with more exaggerated colours.

Coefficients	Estimate ± SE	t-value	P-value
Intercept	0.025 ± 0.048	0.521	0.61
PC1	0.208 ± 0.115	1.803	0.079
PC2	0219 ± 0.121	1.814	0.077

Table 1.2. Partial RDA with permutation tests (999 permutations) on greenness and blackness for the 43 IT populations with genetic data. The results test the statistical significance of the unique fractions explained by climate (PC1 and PC2), the linear trend (x and y coordinates), and spatial structure (dbMEMs).

Unique climate

Model: rda(X = Greenness and Blackness, Y = Climate, Z = cbind(Coordinates, dbMEMs))

	Df	Variance	F	Pr(>F)
Model	2	0.089	2.69	0.05
Residual	36	0.600		

Unique linear trend

Model: rda(X = Greenness and Blackness, Y = Coordinates, Z = cbind(Climate, dbMEMs))

	Df	Variance	F	Pr(>F)
Model	2	0.246	7.36	0.004
Residual	36	0.600		

Unique spatial structure

Model: rda(X = Greenness and Blackness, Y = dbMEMs, Z = cbind(Climate, Coordinates))

	Df	Variance	F	Pr(>F)
Model	2	0.326	9.79	0.001
Residual	36	0.600		

Table 1.3. Partial RDA with permutation tests (999 permutations) on greenness and blackness for the 43 IT populations with genetic data. The results test the statistical significance of the unique fractions explained by climate (PC1 and PC2), genetic distance (Axis 1-3), and spatial structure (dbMEMs).

Unique climate

Model: rda(X = Greenness and Blackness, Y = Climate, Z = cbind(Coordinates, dbMEMs))

	Df	Variance	F	Pr(>F)
Model	2	0.134	3.63	0.02
Residual	35	0.644		

Unique genetic distance

Model: rda(X = Greenness and Blackness, Y = Genetic Distance, Z = cbind(Climate, dbMEMs))

	Df	Variance	F	Pr(>F)
Model	2	0.203	3.68	0.001
Residual	35	0.644		

Unique spatial structure

Model: rda(X = Greenness and Blackness, Y = dbMEMs, Z = cbind(Climate, Coordinates))

	Df	Variance	F	Pr(>F)
Model	2	0.260	7.06	0.001
Residual	35	0.644		

Fig. 1.1. Location of the 43 populations with genetic data belonging to the IT lineage.

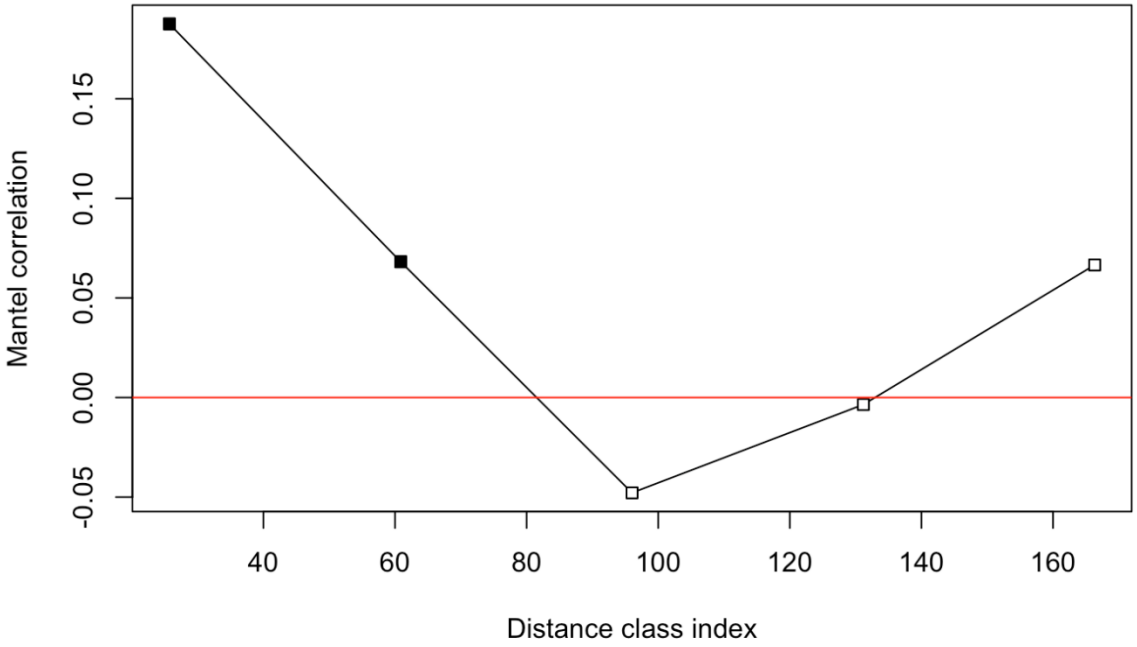

Fig. 1.2. Mantel correlogram for the detrended greenness and blackness data for Italian lineage. The distance on the x-axis is in kilometres. Significant multivariate spatial autocorrelation is indicated by the black squares.

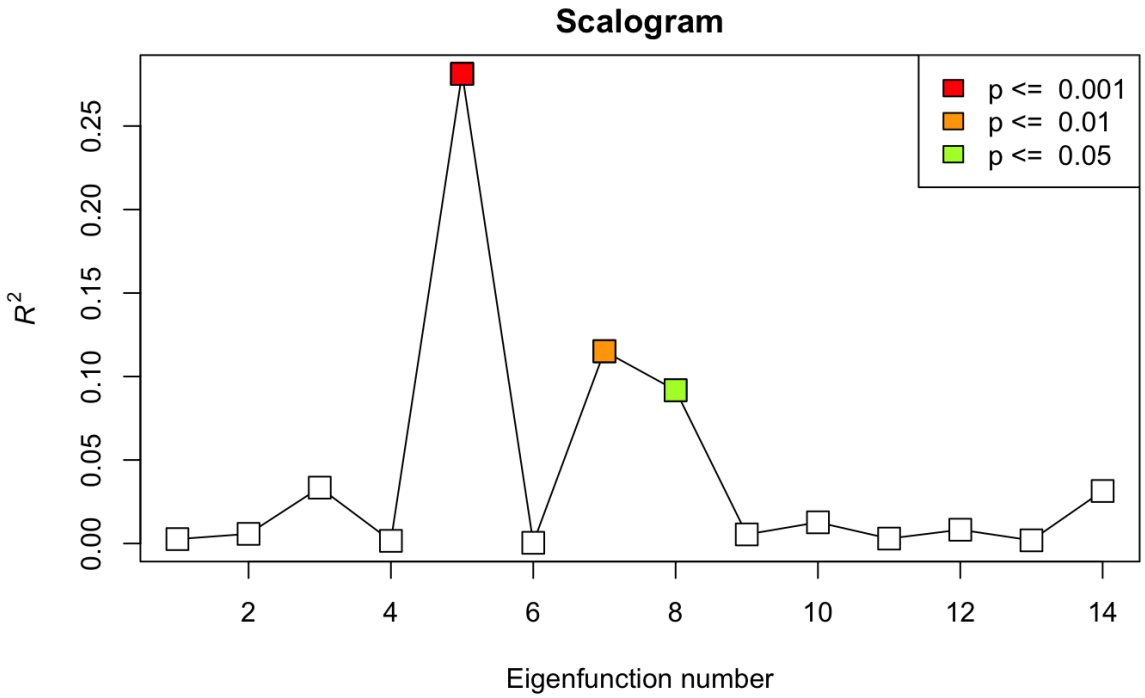

Fig. 1.3. Scalogram for the Italian (IT) lineage. The scalogram shows the explained variance (unadjusted R^2) of the detrended greenness and blackness data explained by the dbMEM eigenfunctions. Colours indicate significance tests based on permutations. Note that dbMEM8 is statistically significant, but not consistently retained in forward simulations.

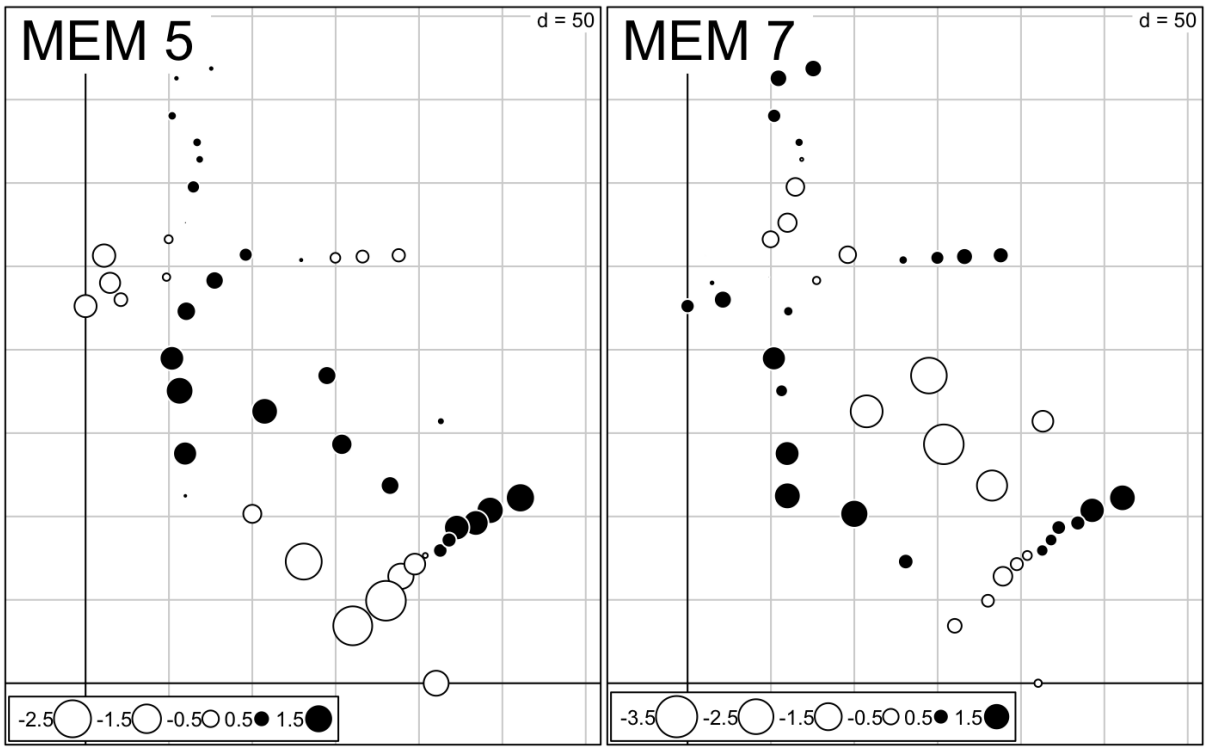

Fig 1.4. The two significant dbMEM variables (retained following forward selection) with positive spatial autocorrelation on the greenness and blackness data for the Italian (IT) lineage. The dbMEMs are ordered from broad to fine spatial scale. Plotted are the scores for each population, indicated by the colour and size of the dots (white = negative, black = positive). The grid indicates the geographic distance (d = 50km).

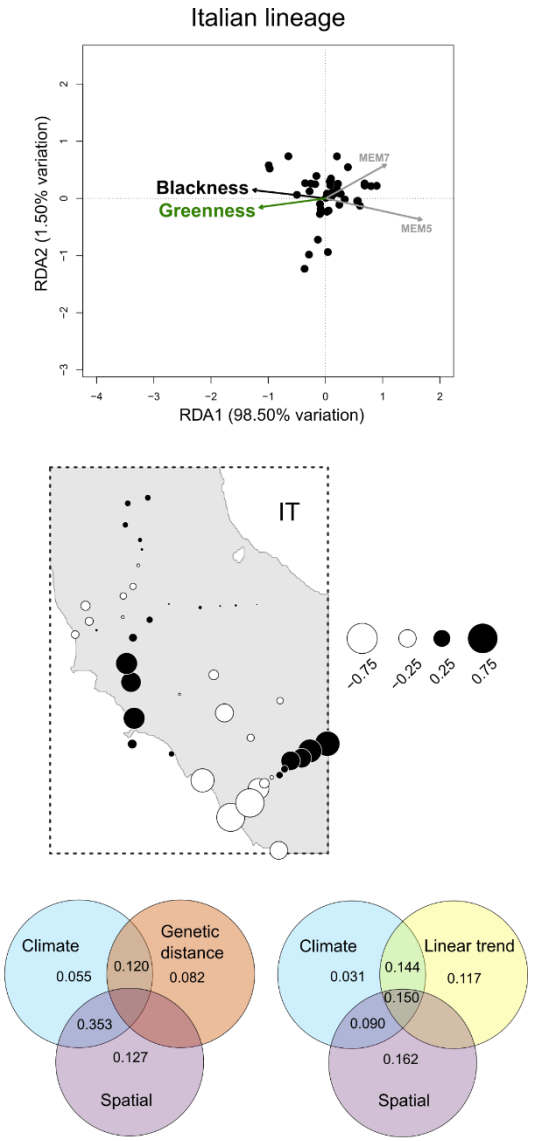

Fig 1.5. Results from the dbMEM analyses for 43 populations belonging to the Italian (IT) lineage. Top: RDA triplots with two canonical axes (RDA1 and RDA2). Black circles represent populations, grey vectors represent the MEM predictors, and green and black vectors the response variables greenness and blackness, respectively. Middle: Fitted scores of the first canonical axis of the redundancy analysis (i.e., RDA1 from top panel). Each dot represents a population; the size and colour of the dots indicate the fitted score of RDA1, with white dots representing negative, and black dots representing positive, scores. For interpretation on its relationship to greenness and blackness, compare with the plots in the top

row (e.g., for the IT lineage in (A), populations represented by large white dots on the map are those with the most intense green-and-black phenotype). Bottom: Variance partitioning of the colouration data with unique and shared fractions of explained variation. Empty fractions were estimated to have zero variance. The Venn diagram on the left shows results for the analysis including genetic distance and the Venn diagram to the right shows results for analysis including the linear trend (i.e., exactly analogous to the results presented in the main text but for 43, instead of 58, populations).

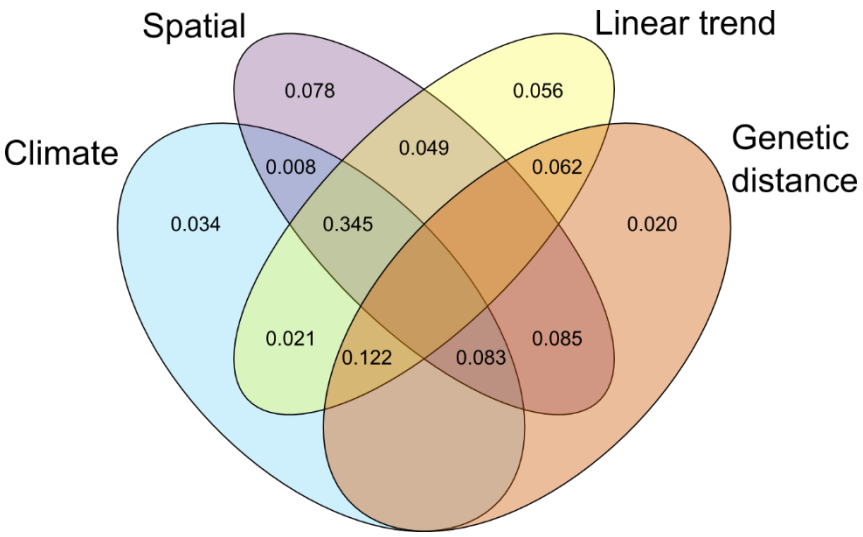

Fig. 1.6. Variance partitioning of the colouration data with unique and shared fractions of explained variation for all four predictors. Empty fractions were estimated to have zero variance. Note that the linear trend and genetic distance are highly collinear, and that the significance of unique and shared fractions therefore were evaluated statistically in models with either genetic distance or the linear trend (see tables 2 and 3, and figure 5).

2. Supplementary Tables

Supplementary tables S1-S7

Table S1. Summary of sampling locations, the number of males included in the phenotypic analyses, and the ancestry (estimated from RAD-seq data or inferred based on the location of the hybrid zone; see Results). These data are also available in .xls as Supplementary File 3. Individual-level phenotypic data is found in Supplementary File 1.

Population ID	Sampling Location	Latitude	Longitude	Number of Males	Population Genetic Data	Ancestry
AC	Altrocanto	42,4807	12,5736	15	Y	IT
AL	Cerreto Alpi	44,3225	10,2509	13	N	MIXED
AR	Arni	44,0682	10,2494	13	Y	MIXED
AS	Assergi	42,4144	13,5090	13	Y	IT
ASS	Abbadia San Salvatore	42,8813	11,6739	13	Y	IT
BC	Bacchereto	43,8100	10,9851	11	Y	IT
BD	Bardi	44,6335	9,7314	18	N	SA
BE	Belforte all'isauro	43,7168	12,3761	15	Y	IT
BF	Brignano-Frascata	44,8135	9,0410	13	Y	SA
BI	Bibbiena	43,6954	11,8201	12	N	IT
BL	Badia Tedalda	43,7100	12,1813	15	Y	IT
BO	Bratto	44,4541	9,8481	17	Y	SA
BT	Buti	43,7266	10,5854	24	N	IT
BZ	Borzonasca	44,4202	9,3895	15	Y	SA
CA	Calci	43,7219	10,5220	29	Y	IT
CB	Castelnuovo Berardenga	43,3445	11,4987	5	N	IT
CD	Certaldo	43,5477	11,0415	8	N	IT

CE	Cento	44,7315	11,2908	13	Y	IT
CHI	Chiavari	44,3177	9,3224	13	Y	SA
CL	Castelfiorentino	43,6058	10,9697	6	Y	IT
CM	Campodimele	41,3818	13,5338	11	N	IT
CN	Chianni	43,4842	10,6425	36	Y	IT
COL	Colle	44,1119	10,3667	16	Y	MIXED
COR	Corbara	42,7033	12,2276	10	Y	IT
CP	Cantolupo	44,8634	8,5529	16	N	SA
CR	Crespina	43,5748	10,5649	15	Y	IT
CT	Castellarano	44,5133	10,7332	19	Y	MIXED
CV	Chiusi della Verna	43,6981	11,9360	6	Y	IT
CX	Cedogno	44,5331	10,3408	12	Y	MIXED
DS	Colle di Sassa	42,3468	13,2917	15	Y	IT
FDM	Forte di Marmi	43,9778	10,2027	16	Y	MIXED
FG	Fagge	42,2786	13,1889	12	Y	IT
FM	Fiumalbo	44,1656	10,6388	16	N	MIXED
FO	Fogliano	41,4133	12,9043	14	Y	IT
FU	Castel Fusano	41,7234	12,3061	23	Y	IT
GC	Greve in Chianti	43,5876	11,3148	26	Y	IT
GN	Genova Nervi	44,3835	9,0460	13	Y	SA
GO	Sesta Godano	44,2910	9,6732	15	N	SA
GR	Gragnola	44,1918	10,1064	20	N	MIXED
IS	Isola Santa	44,0661	10,3146	17	N	MIXED
LC	Santa Lucia	41,9908	12,6516	16	Y	IT
LE	Levanto	44,1686	9,6107	65	Y	SA
LO	Loano	44,1296	8,2568	5	Y	SA
LP	Lago di Pontecosi	44,1343	10,3873	14	Y	MIXED
LS	Lago del Salto	42,2540	13,0521	20	Y	IT
MA	Maremma	42,6535	11,1032	18	Y	IT

MAZ	Manziana	42,1045	12,0991	13	N	IT
MDL	Madonna Dell'Acqua	43,7393	10,3801	9	N	IT
ME	Mele	44,4432	8,7480	16	Y	SA
MF	Monteflavio	42,1030	12,8265	12	Y	IT
MG	Montignoso	44,0122	10,1616	23	Y	MIXED
MM	Montemassi	42,9922	11,0639	8	Y	IT
MOA	Montalto	42,3279	11,5855	16	Y	IT
MP	Monte Penna	44,0926	11,1626	18	Y	IT
MT	Montecatini Terme	43,8941	10,7904	14	N	IT
MV	Monte Acuto Valese	44,2412	11,2080	16	Y	IT
NL	Noli	44,2063	8,4142	19	Y	SA
NO	Nonantola	44,6789	11,0412	15	Y	IT
OL	Olina	44,3050	10,7823	7	N	MIXED
OT	Ottone	44,6240	9,3317	15	N	SA
OV	Orvinio	42,1300	12,9339	9	Y	IT
PA	Pellegrino in Alpe	44,1893	10,4816	17	Y	MIXED
PB	Passo del Bocco	44,4154	9,4435	18	Y	SA
PE	Peccoli	43,5445	10,7201	32	N	IT
PG	Pellegrino Parmesse	44,7332	9,9255	13	N	SA
PGM	Poggio Moiano	42,1863	12,8771	42	N	IT
PI	Perino	44,8198	9,5029	13	Y	SA
PM	Pontremoli	44,3777	9,8817	17	N	SA
PN	Ponteceno	44,5398	9,6025	12	N	SA
POR	Porrona	42,9107	11,4082	6	N	IT
PR	Prato	43,8995	11,1058	14	Y	IT
PS	Palombara Sabina	42,0565	12,7512	17	Y	IT
PT	Prunetta	44,0078	10,8037	15	Y	MIXED
PV	Pian di Venoia	44,3331	11,1894	11	Y	IT
PX	Paganico	42,1867	12,9971	9	Y	IT

QC	Quercianella	43,4494	10,3892	16	Y	IT
RA	Rapallo	44,3494	9,2338	28	Y	SA
RG	San Romano in Garfagnana	44,1699	10,3470	13	N	MIXED
RM	Monte Ramaceto	44,4278	9,3171	16	N	SA
RO	Rome (Via Appio)	41,8586	12,5442	8	Y	IT
RT	Roccotagliata	44,4729	9,1996	16	N	SA
SA	Santo Stefano D'aveto	44,5473	9,4514	12	N	SA
SAR	Sant'Arcangelo	43,0743	12,1206	13	Y	IT
SB	San Bernardo	44,3962	8,4784	5	N	SA
SD	Silvano D'orba	44,6864	8,6729	13	N	SA
SF	Santa Fiora	42,8324	11,5846	14	N	IT
SL	Sestri Levante	44,2714	9,4094	20	Y	SA
SM	San Martino	44,3906	8,5155	13	Y	SA
SMA	Santa Marinella	42,0703	11,9543	14	Y	IT
SO	Sassello	44,4795	8,4902	15	Y	SA
SR	San Remo	43,8183	7,7729	15	N	SA
SS	Sassalbo	44,2883	10,1932	19	N	MIXED
SST	Santo Stefano	42,4250	11,1050	16	Y	IT
ST	San Terenzo	44,1221	9,9658	19	Y	SA
STO	Santa Maria del Toro	44,4337	9,4915	13	N	SA
SU	Subiaco	41,9237	13,0973	12	N	IT
SX	Saltino	43,7267	11,5382	21	Y	IT
TE	Temossi	44,4649	9,3673	15	N	SA
TI	Tirli	42,8438	10,8916	17	N	IT
TM	Tombeto	43,9797	10,5447	13	N	MIXED
TO	Torriglia	44,5189	9,1571	10	Y	SA
TP	Torpiana	44,3107	9,7319	14	N	SA
TR	Travale	43,1674	11,0084	12	Y	IT

TZ	Triponzo	42,8278	12,9382	15	Y	IT
UR	Urbino	43,7236	12,6359	13	Y	IT
US	Uscio	44,4152	9,1563	27	N	SA
VA	Varazze	44,3592	8,5774	22	Y	SA
VE	Colle Di Val D'Elsa	43,4215	11,1118	23	Y	IT
VG	Vignola	44,4763	11,0105	8	Y	IT
VI	Viareggio	43,8427	10,2633	31	Y	MIXED
VO	Vaggio	43,6407	11,5072	5	N	IT
VS	Vagli Sopra	44,1184	10,2663	13	N	MIXED
VZ	Valmozzola	44,5821	9,9421	27	N	SA
ZE	Zeri	44,3527	9,7639	12	N	SA

Table S2. Loadings for the first two principal components on the bioclimatic variables. The first two PCs, explaining 79.5% of the variation, were statistically significant in a broken stick model and used in all subsequent modelling.

Bioclimatic variable	**PC1**	**PC2**
BIO1 = Annual Mean Temperature	**-0,3**	-0,1
BIO2 = Mean Diurnal Range (Mean of monthly (max temp - min temp))	-0,1	**0,32**
BIO3 = Isothermality (BIO2/BIO7) (×100)	-0,1	0,1
BIO4 = Temperature Seasonality (SD ×100)	-0,1	**0,41**
BIO5 = Max Temperature of Warmest Month	**-0,3**	0,04
BIO6 = Min Temperature of Coldest Month	-0,2	**-0,3**
BIO7 = Temperature Annual Range (BIO5-BIO6)	-0,1	**0,41**
BIO8 = Mean Temperature of Wettest Quarter	**-0,3**	0,01
BIO9 = Mean Temperature of Driest Quarter	-0,1	**-0,3**
BIO10 = Mean Temperature of Warmest Quarter	**-0,3**	-0
BIO11 = Mean Temperature of Coldest Quarter	**-0,3**	**-0,3**
BIO12 = Annual Precipitation	**0,29**	-0,1
BIO13 = Precipitation of Wettest Month	**0,27**	-0,2
BIO14 = Precipitation of Driest Month	**0,28**	0,15
BIO15 = Precipitation Seasonality (CV)	-0	**-0,4**
BIO16 = Precipitation of Wettest Quarter	**0,28**	-0,2
BIO17 = Precipitation of Driest Quarter	**0,29**	0,04
BIO18 = Precipitation of Warmest Quarter	**0,29**	0,06
BIO19 = Precipitation of Coldest Quarter	**0,27**	-0,2

Table S3. Partial RDA with permutation tests (999 permutations) on greenness and blackness for the Italian (IT) lineage. The results tests the statistical significance of the unique fractions explained by climate (PC1 and PC2), the linear trend (x and y coordinates), and spatial structure (dbMEMs).

Pure Climate

Model: rda(X = Greenness&Blackness, Y = Climate, Z = cbind(Coordinates, dbMEMs))

	Df	Variance	F	Pr(>F)
Model	2	0.12322	4.7965	0.008
Residual	49	0.62939		

Pure linear trend

Model: rda(X = Greenness&Blackness, Y = Coordinates, Z = cbind(Climate, dbMEM))

	Df	Variance	F	Pr(>F)
Model	2	0.20102	7.8251	0.002
Residual	49	0.62939		

Pure spatial structure

Model: rda(X = Greenness&Blackness, Y = dbMEM, Z = cbind(Climate, Coordinates))

	Df	Variance	F	Pr(>F)
Model	4	0.35120	6.8355	0.001
Residual	49	0.62939		

Table S4. Statistical significance of coefficients in a spatially and spatially non-varying coefficient model of greenness and blackness in the Italian (IT) lineage. Note that the coefficients for climatic PC1 for greenness is estimated to be constant and significant.

	Greenness			Blackness		
	Intercept	PC1	PC2	Intercept	PC1	PC2
Not significant	46	0	34	40	33	58
Significant (10% level)	2	0	2	6	4	0
Significant (5% level)	6	0	9	10	11	0
Significant (1% level)	4	58	13	2	10	0

Table S5. Partial RDA with permutation tests (999 permutations) on greenness and blackness for the Southern Alps (SA) lineage. The results tests the statistical significance of the unique fractions explained by climate (PC1 and PC2), the linear trend (x and y coordinates), and spatial structure (dbMEMs).

unique climate

Model: rda(X = Greenness&Blackness, Y = Climate, Z = cbind(Coordinates, dbMEMs))

	Df	Variance	F	Pr(>F)
Model	1	0.04004	1.9005	0.163
Residual	29	0.61094		

unique linear trend

Model: rda(X = Greenness&Blackness, Y = Coordinates, Z = cbind(Climate, dbMEM))

	Df	Variance	F	Pr(>F)
Model	2	0.44498	10.561	0.001
Residual	29	0.61094		

unique spatial structure

Model: rda(X = Greenness&Blackness, Y = dbMEM, Z = cbind(Climate, Coordinates))

	Df	Variance	F	Pr(>F)
Model	4	0.30398	3.6073	0.006
Residual	29	0.61094		

Table S6. Statistical significance of coefficients in a spatially and spatially non-varying coefficient model of greenness and blackness in the Southern Alps (SA) lineage.

	Greenness			Blackness		
	Intercept	PC1	PC2	Intercept	PC1	PC2
Not significant	37	37	12	36	37	37
Significant (10% level)	0	0	5	1	0	0
Significant (5% level)	0	0	4	0	0	0
Significant (1% level)	0	0	16	0	0	0

Table S7. Partial RDA with permutation tests (999 permutations) on greenness and blackness for the hybrid zone. The results tests the statistical significance of the unique fractions explained by climate (PC1 and PC2) and the linear trend (x and y coordinates). There was no overall significant spatial structure (dbMEMs).

unique climate

Model: rda(X = Greenness&Blackness, Y = Climate, Z = cbind(Coordinates))

	Df	Variance	F	Pr(>F)
Model	2	0.34861	2.3774	0.085 .
Residual	14	1.02644		

unique linear trend

Model: rda(X = Greenness&Blackness, Y = Coordinates, Z = cbind(Climate))

	Df	Variance	F	Pr(>F)
Model	2	0.2219	1.5133	0.245
Residual	14	1.0264		

3. Supplementary Figures

Supplementary figures S1-S14

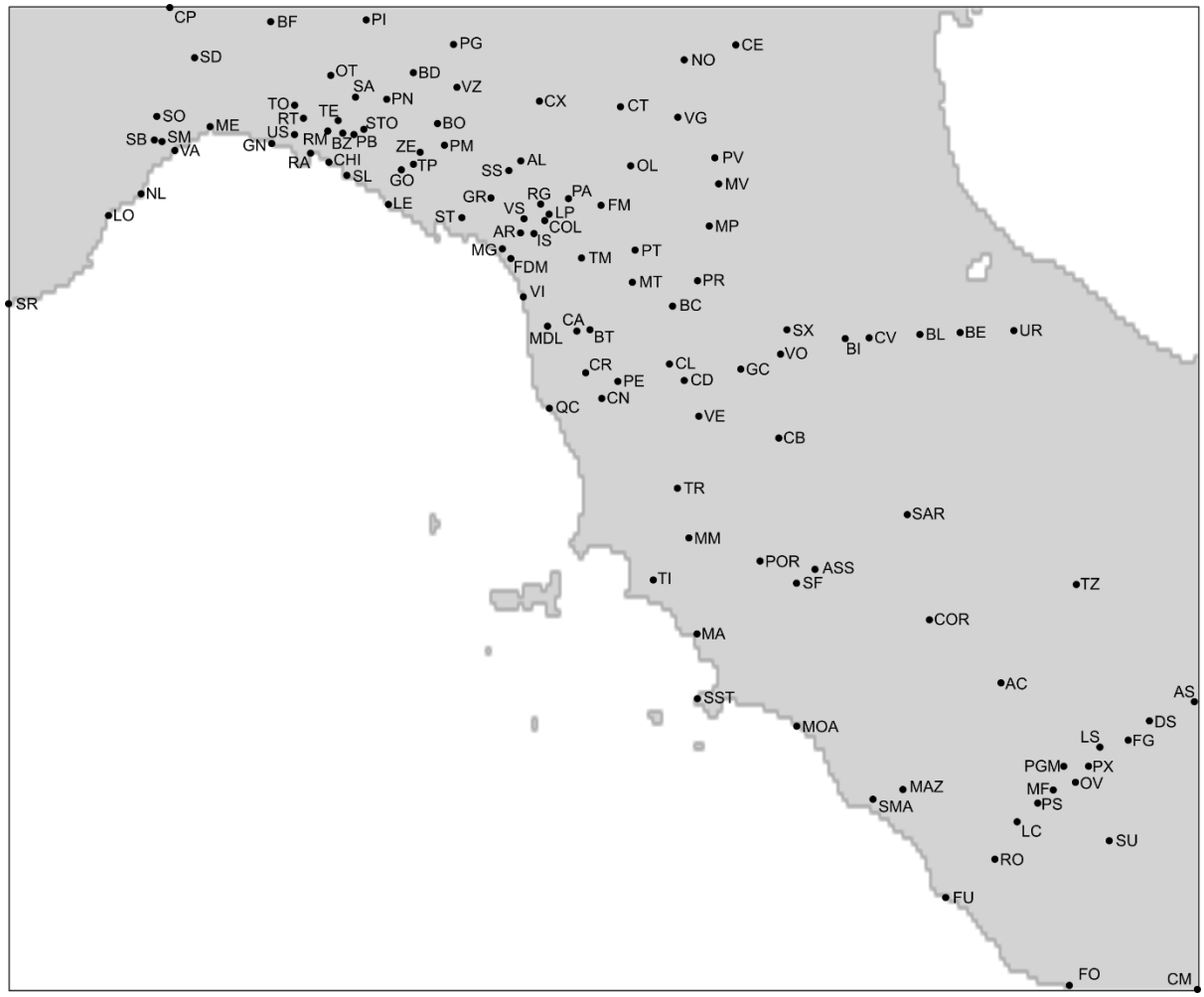

Fig. S1. Map of study locations with population abbreviations.

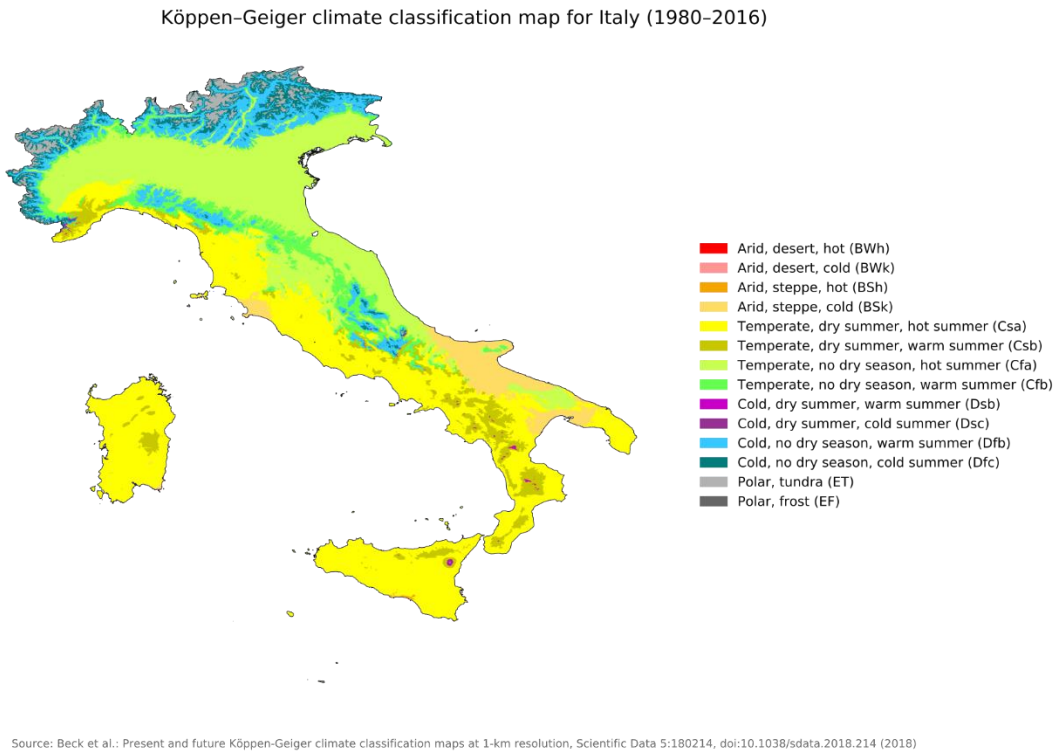

Fig. S2. Köppen-Geiger climate classification map for Italy (from Beck et al. 2018). Licensed under creative commons (CC BY 4.0). Beck, Hylke E.; Zimmermann, Niklaus E.; McVicar, Tim R.; Vergopolan, Noemi; Berg, Alexis; Wood, Eric F. 2018. Present and future Köppen-Geiger climate classification maps at 1-km resolution. *Scientific Data*. **5**: 180214. doi:10.1038/sdata.2018.214

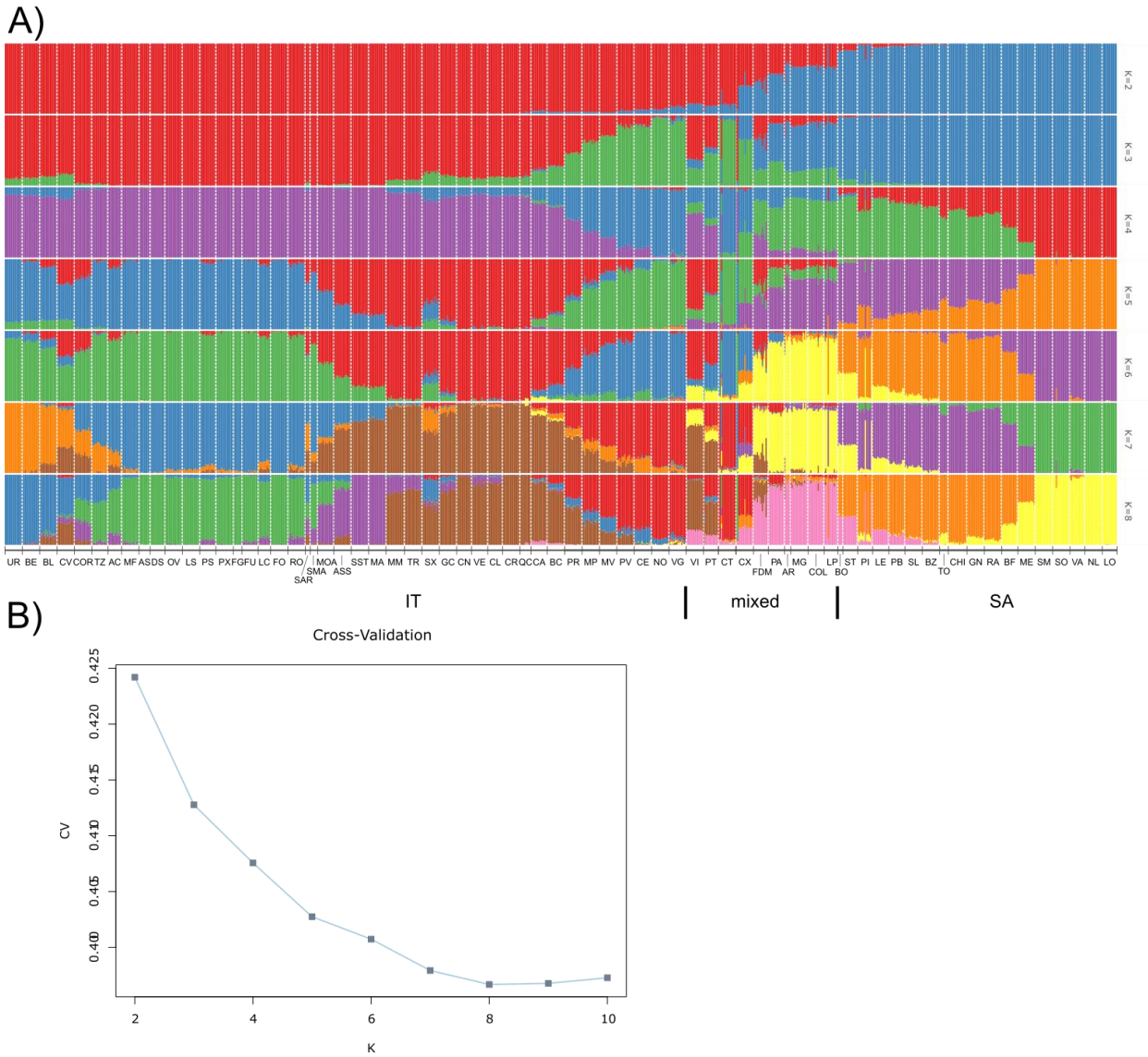

Fig. S3. (A) Results from the ADMIXTURE analysis for different number of clusters, K=2-8. Colours of the ADMIXTURE plot indicate genetic clusters. (B) Cross-validation for K = 2-10.

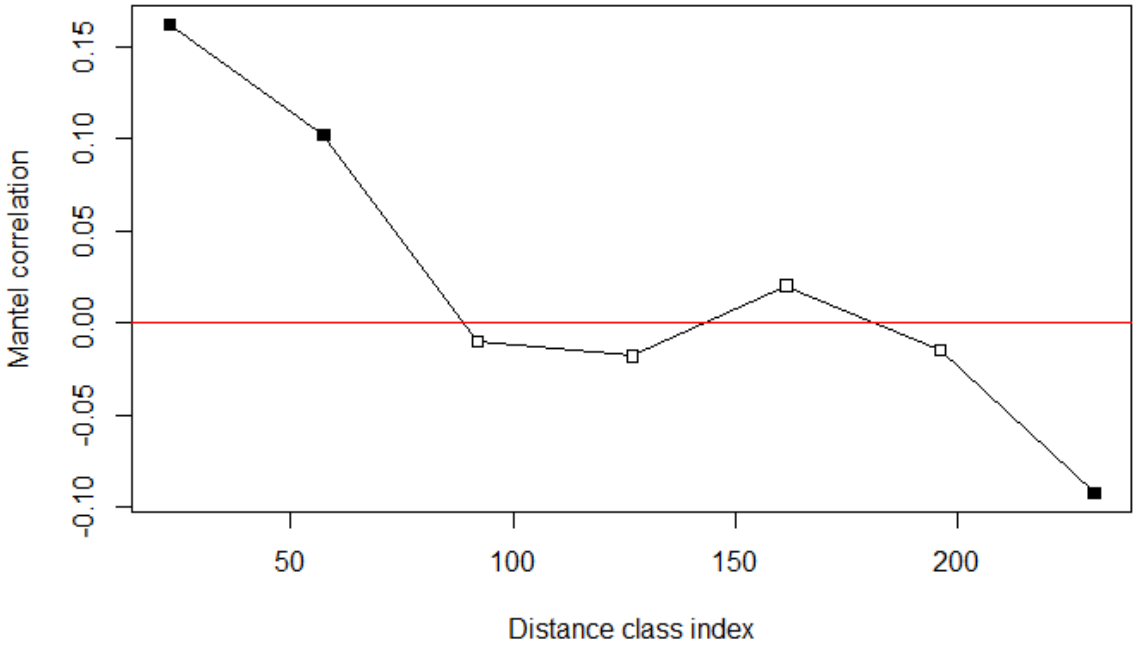

Fig. S4. Mantel correlogram for the detrended greenness and blackness data for the Italian (IT) lineage. The distance on the x-axis is in kilometres. Significant multivariate spatial autocorrelation is indicated by the black squares.

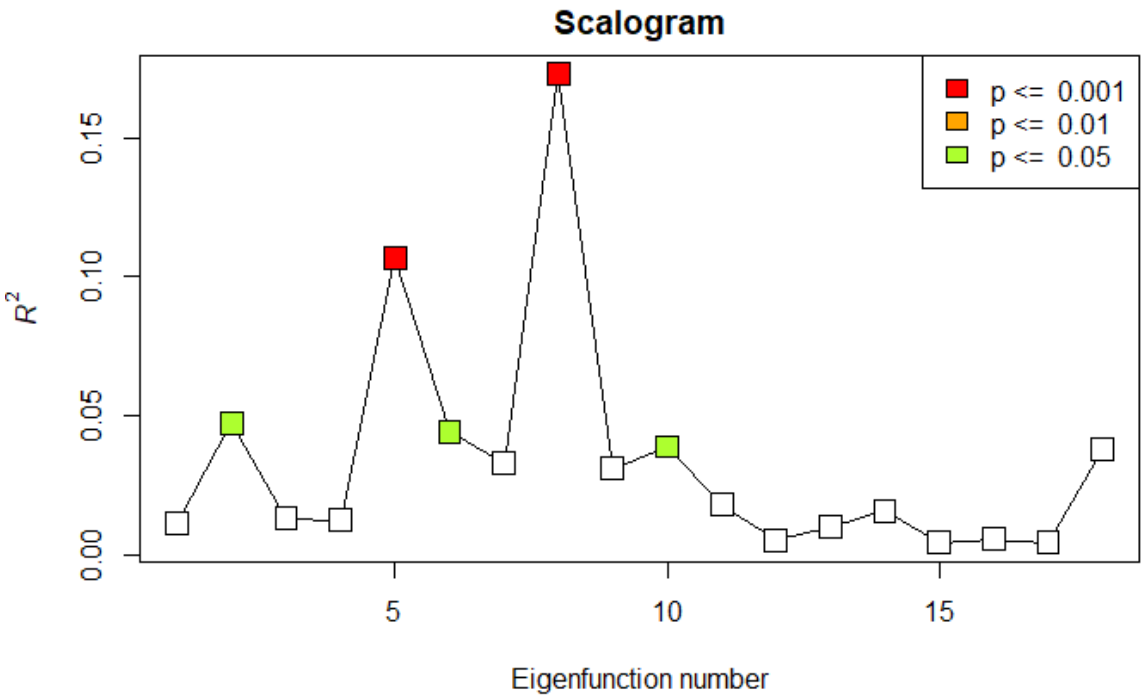

Fig. S5. Scalogram for the Italian (IT) lineage. The scalogram shows the explained variance (unadjusted R^2) of the detrended greenness and blackness data explained by the dbMEM eigenfunctions. Colours indicate significance tests based on permutations. Note that MEM10 is statistically significant but not consistently retained in forward simulations.

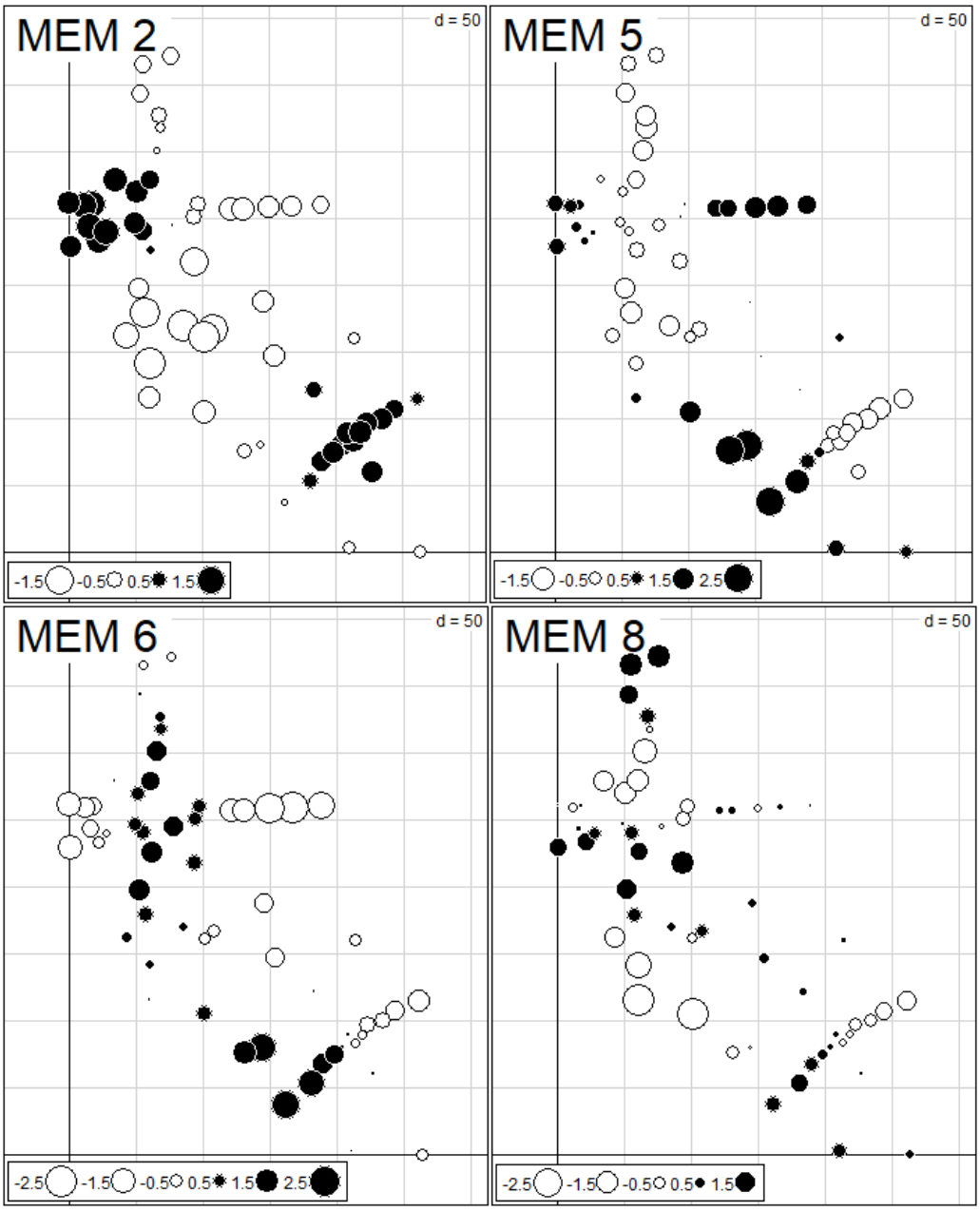

Fig. S6. The four significant dbMEM variables (retained following forward simulation) with positive spatial autocorrelation on the greenness and blackness data for the Italian (IT) lineage. The MEMs are ordered from broad to fine spatial scale. Plotted are the scores for each population, indicated by the colour and size of the dots (white = negative, black = positive). The grid indicates the geographic distance (d = 50km).

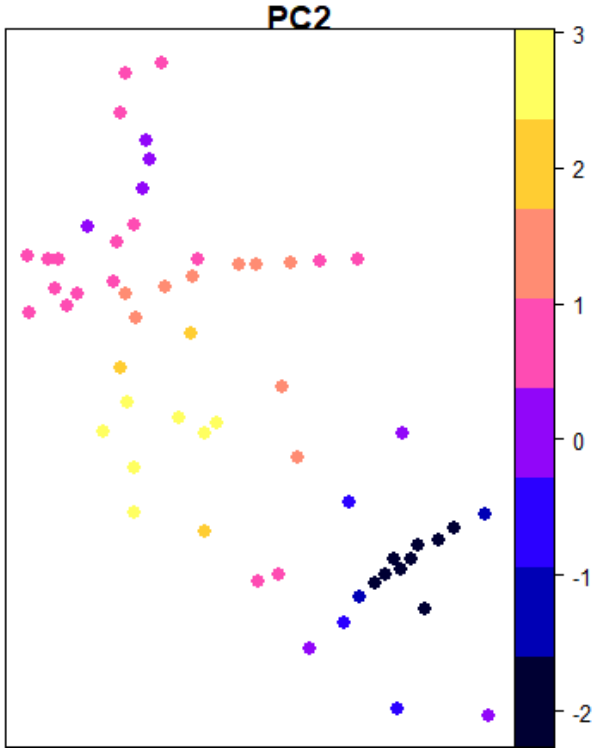

Fig. S7. Output from a spatially varying and non-varying coefficient model of greenness in the Italian lineage. The map shows the estimated coefficients for climatic PC2 from a random regression with standardized greenness as the dependent variable, climatic PC1 and PC2 as explanatory variables, and controlling for the spatial connectivity using the forward-selected Moran eigenvectors. The coefficients for PC1 was estimated to be constant. The results demonstrate that PC2 has a particularly strong negative effect north-east from Rome (towards the Apennines), and a positive effect along the coast. See Table S4 for a summary of statistical significance of the spatially varying coefficients.

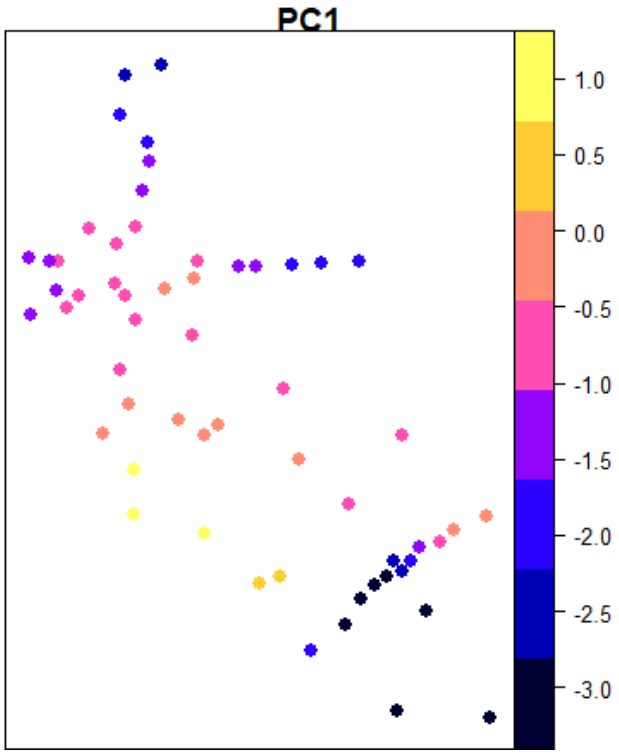

Fig. S8. Output from a spatially varying and non-varying coefficient model of standardized blackness in the Italian lineage. The map shows the estimated coefficients for climatic PC1 from a random regression with standardized blackness as the dependent variable, climatic PC1 and PC2 as explanatory variables, and controlling for the spatial connectivity using the forward-selected Moran eigenvectors. The coefficient for PC2 was not significant. The results demonstrate that PC1 has a particularly strong negative effect north-east from Rome (towards the Apennines), but a positive effect along the coast. See Table S4 for a summary of statistical significance of the spatially varying coefficients.

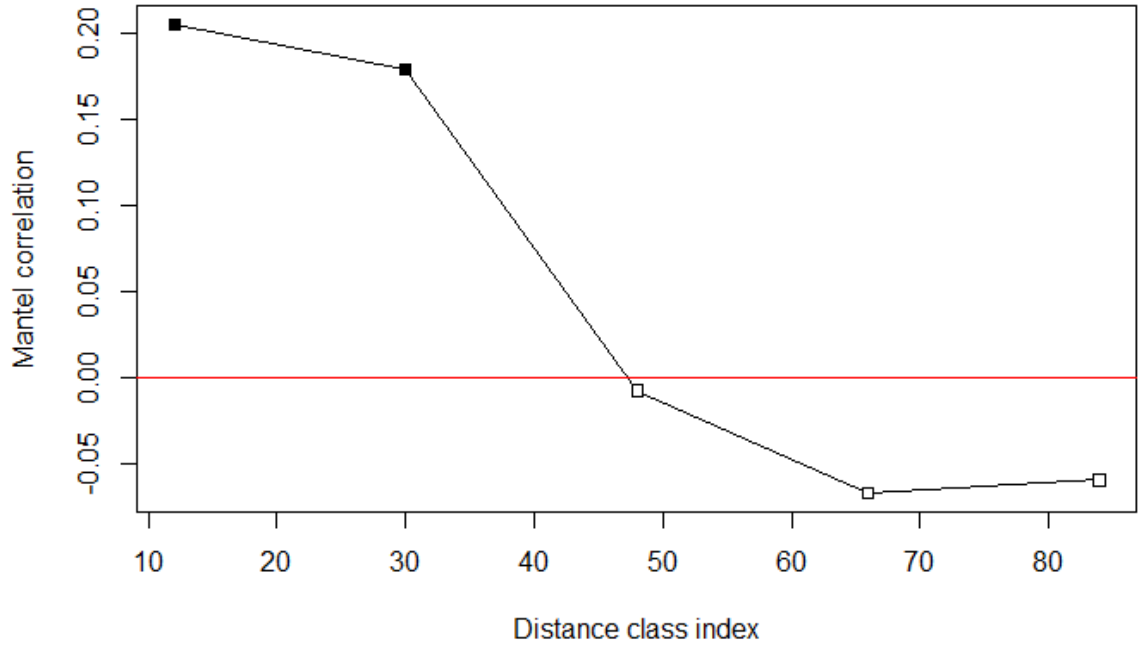

Fig. S9. Mantel correlogram for the detrended greenness and blackness data for the Southern Alps (SA) lineage. The distance on the x-axis is in kilometers. Significant multivariate spatial autocorrelation is indicated by the black squares.

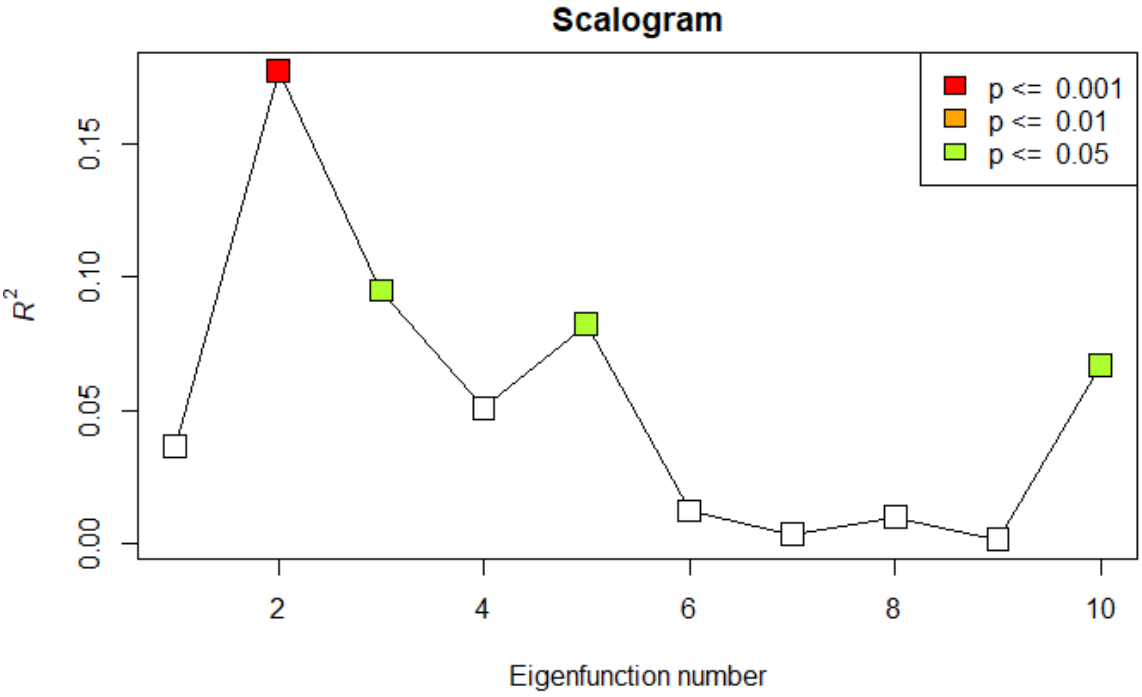

Fig. S10. Scalogram for the Southern Alps (SA) lineage. The scalogram shows the explained variance (unadjusted R^2) of the detrended greenness and blackness data explained by the dbMEM eigenfunctions. Colours indicate significance tests based on permutations.

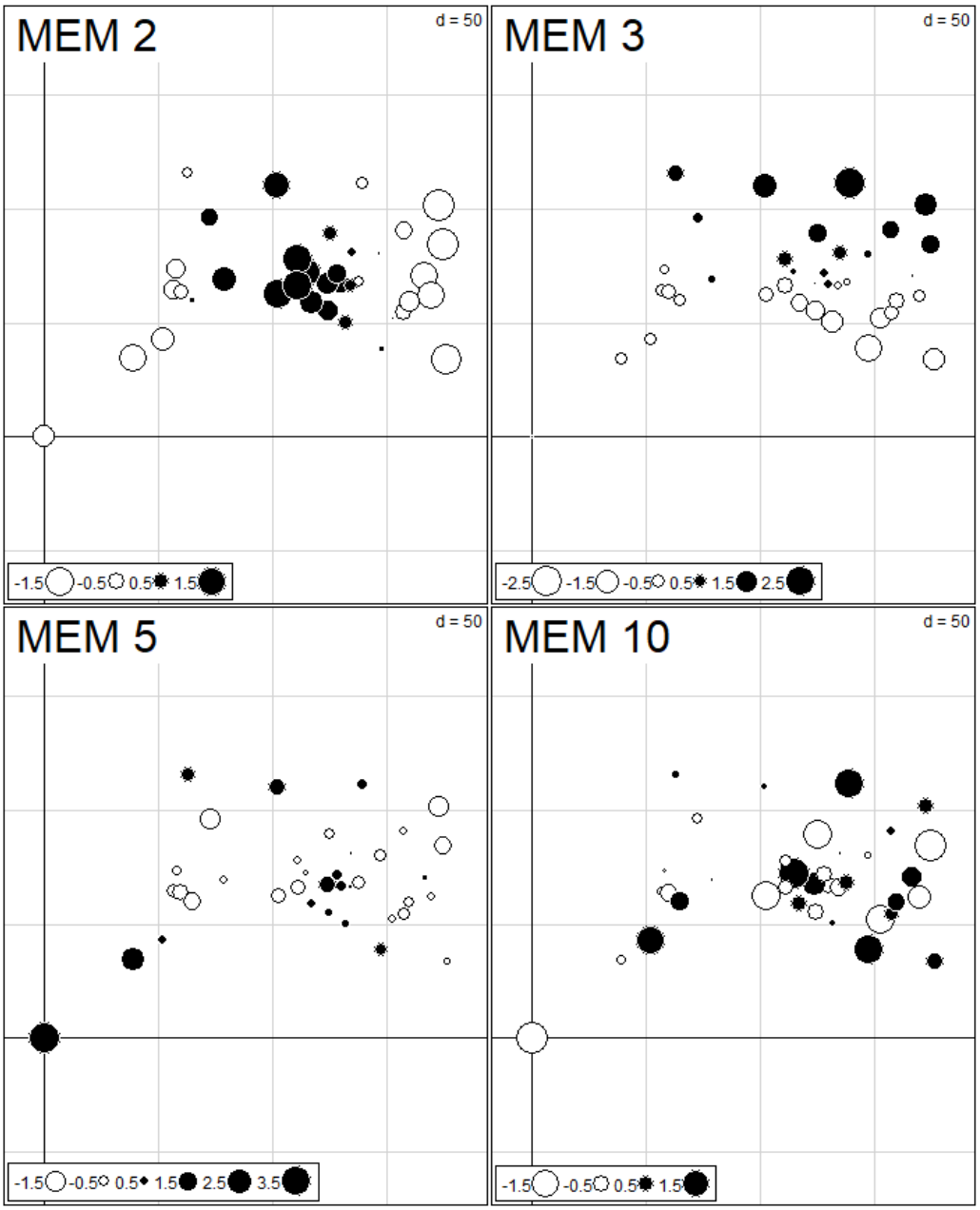

Fig. S11. The four significant dbMEM variables (retained following forward simulation) with positive spatial autocorrelation on the greenness and blackness data for the Southern Alps (SA) lineage. The MEMs are ordered from broad to fine spatial scale. Plotted are the scores for each population, indicated by the colour and size of the dots (white = negative, black = positive). The grid indicates the geographic distance (d = 50km).

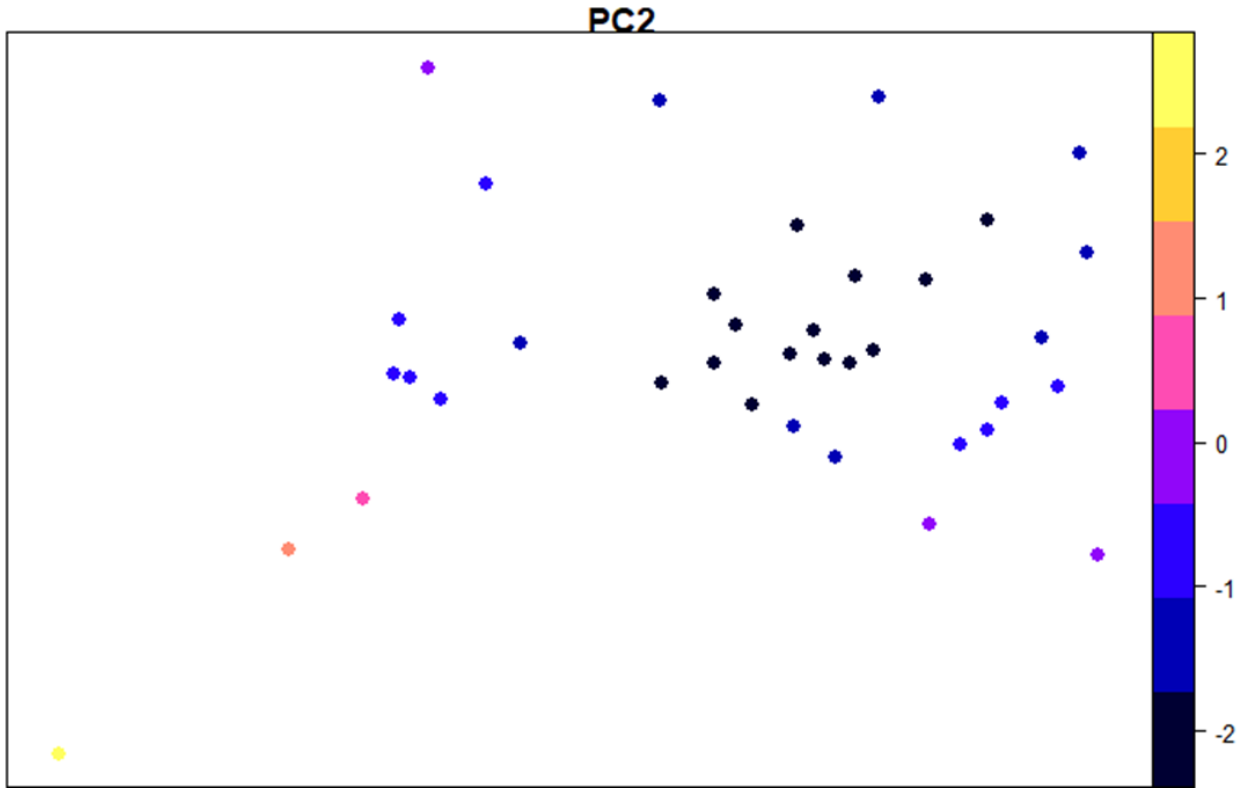

Figure S12. Output from a spatially varying and non-varying coefficient model of standardized greenness in the Southern Alps lineage. The map shows the estimated coefficients for climatic PC2 from a random regression with standardized greenness as the dependent variable, climatic PC1 and PC2 as explanatory variables, and controlling for the spatial connectivity using the forward-selected Moran eigenvectors. The coefficient for PC1 was borderline statistically significant. The results demonstrate that the coefficient for PC2 switches from negative to positive far west, which illustrates that the colouration has not yet reached all the regions where it is likely to be under positive selection. See Table S6 for a summary of statistical significance of the spatially varying coefficients.

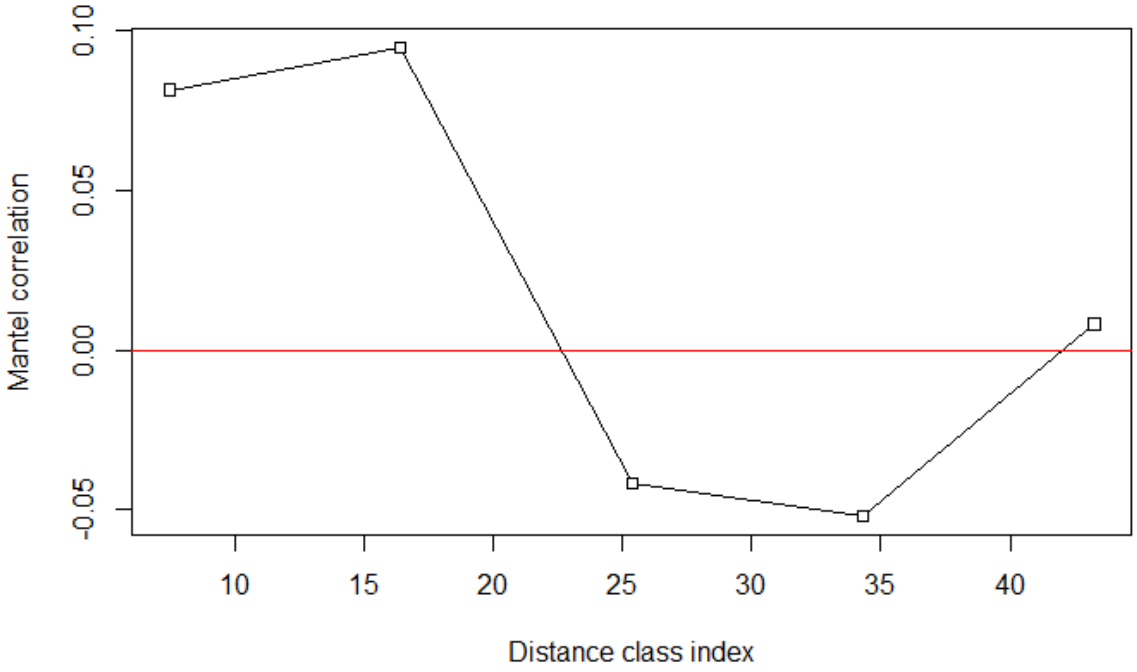

Fig. S13. Mantel correlogram for the detrended greenness and blackness data for the hybrid zone. The distance on the x-axis is in meters. None of the multivariate spatial autocorrelations are significant after correction for multiple testing.

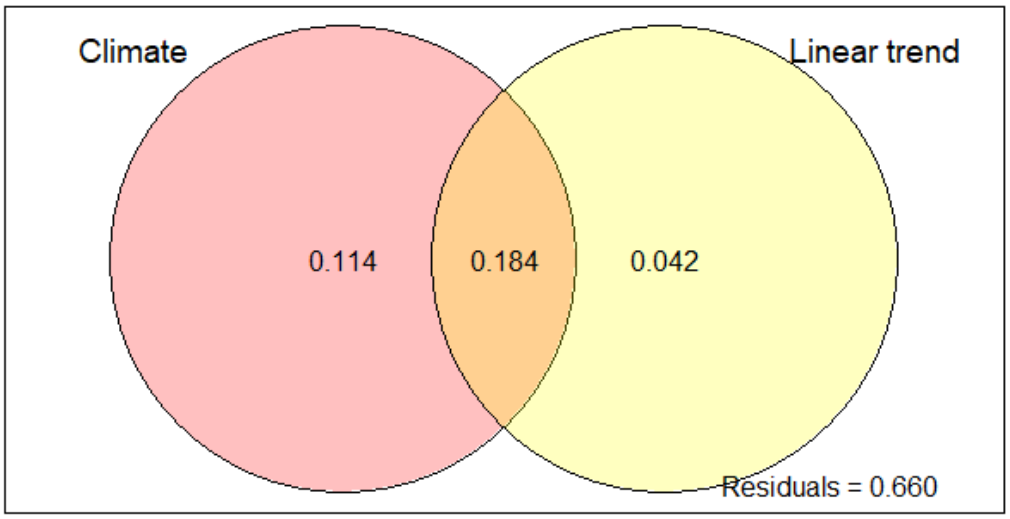

Fig. S14. Variation partitioning of the greenness and blackness data for the hybrid zone. The variation is separated into a climatic (PC1 and PC2) component and a linear trend. There was no further spatial structure within the hybrid zone. While both climate and the linear trend were statistically significant (see Results), the unique fractions of variance explained did not reach statistical significance (Table S7).